A THEORETICAL PERFORMANCE INVESTIGATION OF AN AFTERBURNING TURBOFAN ENGINE

JAMES F. BELL

A THEORETICAL PERFORMANCE INVESTIGATION OF AN AFTERBURNING TURBOFAN ENGINE

*****

James F. Bell

A THEORETICAL PERFORMANCE INVESTIGATION OF AN AFTERBURNING TURBOFAN ENGINE

by

James F. Bell
Lieutenant, United States Navy

Submitted in partial fulfillment of
the requirements for the degree of

MASTER OF SCIENCE

IN

AERONAUTICAL ENGINEERING

United States Naval Postgraduate School
Monterey, California

1962

A THEORETICAL PERFORMANCE INVESTIGATION OF AN AFTERBURNING TURBOFAN ENGINE

by

James F. Bell

This work is accepted as fulfilling
the thesis requirements for the degree of

MASTER OF SCIENCE
IN
AERONAUTICAL ENGINEERING

from the

United States Naval Postgraduate School

ABSTRACT

This study presents results of a theoretical evaluation of the performance of an afterburning turbofan engine when used for high altitude, high speed flight. The calculated performance is compared with that of a conventional turbojet, and also a combination ram-turbojet, by means of the performance parameters of specific fuel consumption and specific thrust. As the study involved a considerable amount of calculations, the problem was coded in Fortran computer language by the writer. The results of the study were generated by the Control Data Corporation model 1604 digital computer of the Postgraduate School. The results of the study indicate that above Mach 2 the afterburning turbofan shows an increasing performance advantage with increasing Mach number and altitude over the turbojet engine.

The work was conducted at the U. S. Naval Postgraduate School, Monterey, California.

TABLE OF CONTENTS

TABLE OF FIGURES

1. INTRODUCTION

With our country committed to the development of supersonic cruise aircraft such as the B-70 and the supersonic transport, it is desirable to investigate the relative merits of engines to propel this type aircraft in the Mach 2-3 flight regime from 60,000 to 80,000 feet. The performance of the afterburning turbofan engine was compared to that of a turbojet and also a combination ram-turbojet engine up to and including this flight region. Conventional relationships were used for tracing temperature and pressure values through the various engine components, and efficiencies and temperature limitations throughout the engine were assumed as consistent with the present state of the art in gas turbine development. As the problem involved a considerable amount of calculations, it was programmed for the Model 1604 computer located at the Postgraduate School.

The results of this investigation indicate that there is a definite performance advantage for the afterburning turbofan engine in the Mach 2-3 flight area. The superiority of the turbofan in the subsonic flight regions is already well known and this study indicates that the same engine, modified for main and by-pass section afterburning, should be considered for any aircraft designed to cruise at Mach numbers in excess of Mach 2.

The writer wishes to express his appreciation for the assistance and encouragement given him by Professor M. H. Vavra of the Aeronautics Department of the U. S. Naval Postgraduate School.

2. TABLE OF SYMBOLS

Analysis	Computer Program	
b	B	bleed air, lb air/lb air mass flow
f/a	FA	fuel air ratio, lb fuel/lb air
$\dot{m}$		mass flow rate, pounds per second
n	EN	polytropic process exponent
A		area, square feet
Alt	H	altitude, feet
C_p	CP	specific heat, BTU per pound per ^{o}R
HV		heating value, BTU per pound
M_o	FMN	flight Mach number
P	P	pressure, pounds per square foot
$(P2/P1)_{SL}$	PRSL	compressor pressure ratio at sea level
$(P9/P8)_{SL}$	FPRSL	fan pressure ratio at sea level
N		revolutions per minute
R	R	gas constant, ft-lb per lb ^{o}R
SF1	SF1	specific fuel consumption, main engine section, pound fuel per hour per pound thrust
SF2	SF2	specific fuel consumption, by-pass section, pound fuel per hour per pound thrust
SFC	SFC	total specific fuel consumption, pound fuel per hour per pound thrust
T	T	temperature, degrees Rankine
Th		thrust, pounds
THFS	THFS	non-dimensionalized thrust, by-pass section
THS	THS	non-dimensionalized thrust, main engine section
TS1	TS1	specific thrust, main engine section, pound thrust per pound air per second
TS2	TS2	specific thrust, by-pass section, pound thrust per pound air per second
TST	TST	total specific thrust, pound thrust per pound air per second
V		velocity, feet per second

TABLE OF SYMBOLS (continued)

Analysis	Computer Program	
γ	GAM	specific heat ratio
ζ	ZETAD	pressure recovery factor
μ	BPR	by-pass ratio
Subscripts:		
1,2, etc.	1,2, etc.	stations designated in Fig. 2
AB	AB	afterburner
C	C	compressor
D	D	diffuser
F	F	fan
FAB	FAB	fan afterburner
FT	FT	fan turbine
MB	MB	main burner
NF	NF	fan nozzle
NM	NM	main nozzle

3. ANALYSIS

The turbo-fan jet or bypass engine has come into considerable interest of late with its introduction as the powerplant on virtually every commerical transport designed for a cruise speed in Mach .8-.9 region. The recently unveiled Convair 990 is the first airliner to be designed specifically for a by-pass engine (the others having undergone modification programs to switch to turbofan engines from their initially installed straight jet engines) and is being billed as the fastest airliner in the world. This is not by accident, and at the risk of oversimplification of the problem, one of the primary reasons can be easily seen by a look at the propulsive efficiency equation for a straight jet engine: $\eta_p = \frac{2}{1 + V_j/V_a}$, where V_j is the exhaust velocity and V_a the velocity of the aircraft. Thus, propulsive efficiency is inversely proportional to the velocity of exhaust gases leaving the engine. The turbofan engine makes use of this fact and in essence accelerates a larger mass of air by a smaller average amount with a resultant increase in overall propulsive efficiency in comparison to a straight jet engine.

This fact was realized at an early stage by the pioneers in the jet engine development field and the first patent for a by-pass type engine was actually applied for by Whittle in 1936. The first fan jet engine was built in 1946 by Vickers and the well known Conway engine of Rolls Royce has been in a continuous development stage since 1947. In commercial use today in this country are the CJ-805-23 turbofan built by General Electric with a take-off thrust of 16,100 pounds and the JT3D turbofan built by Pratt and Whitney with a take-off thrust of 18,000 pounds.

It is probably appropriate at this time to stop and review the principles of turbofans and their possible cycles. As was pointed out previously, in comparison to a straight jet engine the turbofan exacts a lower average acceleration to a greater mass of air. The turboprop on the other hand, extracts almost all of the available energy from the exhaust gases and handles a large mass of air with its propeller. Thus

it is seen that the turbofan engine has an operating region lying between that of a turboprop and that of a pure turbojet. This is depicted in general terms in Fig. 1. It is apparent from the figure why the turbofan enjoys its popularity in the high sub-sonic speed region.

Once the obvious virtues of the turbofan as is known today have been brought forth, it is natural to mention a salient feature of the turbofan, that being the multitude of design choices for any particular engine. Whereas for a turbojet the major variables are compressor pressure ratio, turbine inlet temperature and degree of reheat in the afterburner, the turbofan has the additional variables of pressure ratio across the fan and by-pass ratio (mass flow rate of air bypassed/mass flow rate of air through the main engine).

This paper is a study of optimizing these variables of a by-pass turbofan engine as depcited in Fig. 2. This study introduces two additional variables as are shown, that being the capability of afterburning in varying degrees in both the main exhaust and the by-pass section aft of the fan. This study is to establish operational characteristics of this type of engine, in comparison with others, in the Mach 2-3 speed regime at cruise altitudes of 60,000 to 70,000 feet.

It is interesting to note at this point the magnitude of the problem one is confronted with in dealing with an investigation that has a large number of variables. Needless to say, the problem is insurmountable without the aid of a computer, but even with such valuable assistance as the CDC 1604 computer which was used extensively in preparing this paper and is capable of exceptionally fast computation and transfer times, the uninitiated might not immediately recognize the dimensions of the problem. As an example, the variables that entered in this problem were altitude, flight Mach number, compressor pressure ratio, turbine inlet temperature, by-pass ratio, main engine afterburner temperature, fan pressure ratio, and the fan afterburner temperature. For one set of calculations which is included as section D in the Appendix of this report, the turbine inlet temperature was equal to a constant $2000^{\circ}R$, altitude varied from sea level to 80,000 feet at 10,000 foot intervals, flight Mach number, by-pass ratio, fan pressure ratio, compressor pressure ratio, by-pass ratio, main engine

and by-pass afterburner temperatures all had a range of variance of three separate values. To the casual observer of the problem this might seem to be a light treatment since only three values were chosen for each variable. However, this actually amounts to 9 times 3 to the 7th power or 19,683 separate solutions. This particular problem took 17 minutes 56 seconds of computer running time. Allowing the above named variables to assume only one additional value each would have increased the computer running time by a factor of eight or would have made a computer problem of approximately 2 hours and 28 minutes running time. If for no other reason, when one is considering a problem of this scope, the economics of computer operation must be recognized since the time spent on modern high speed computers is valued at $500 an hour and up.

For this reason undoubtedly, and probably for others, there seems to be a limited amount of literature on what appears to be the natural development of the highly efficient turbofan engine of the transonic regime to the thrust augmented afterburning turbo-fan for supersonic flight.

The performance of the turbo-fan is outstanding in the high-subsonic and in the transonic speed regime. The turbo-fan is superior to the turbojet because it accelerates a larger mass of air by a smaller amount. As pointed out previously, this fact results in a higher propulsive efficiency. It is clear however, that such a turbofan has a larger diameter than a turbojet, because of the larger mass flow rate. The additional resistance of the turbofan is not too detrimental in the transonic speed region since engines for such applications can be arranged in pods under the wing, and no undue problems or drawbacks occur because of the slight additional weight and the larger engine diameter. However, when considering relative merits of engines for supersonic flight, it is felt that they must be compared on the basis of equal dimensions, in other words, equal air mass flow rates. In nearly all the proposed designs for aircraft of the supersonic transport type that have been published, the engines are integral with the wing and/or fuselage. That is, nearly all of them are of the B-70 type configuration and thus the engines considered for such an aircraft would be volume or

space limited. It is for this reason, that in this report all comparisons between engines are on the basis of the same mass flow rate.

For this discussion the engine components will be observed one at a time and the assumptions made and equations used in each section will be included under the component heading for that particular section. The equations used for tracing the temperature and pressure values through the engine are the standard commonly accepted ones found in Ref. 1.

Values for the ICAO standard atmosphere (1952) were used in determining ambient temperature and pressure at each altitude. Thus from sea level to 36,089 feet the ambient temperature in degrees Rankine is

$$T_o = [1.0 - 6.8719 \times 10^{-6} (Alt)] 518.7$$

and the ambient pressure in lbs per square foot

$$P = [(1.0 - 6.8719 \times 10^{-6})(Alt)]^{5.2561} \times 2116.2$$

Above the tropopause the values become

$$T_o = 389.98 \text{ R}$$

$$P = e^{-4.8088 \times 10^{-5} (Alt - 36089)} \times 472.68$$

The relationships for the specific heat ratio γ and C_p for combustion of fuel and air up to 3000°R were obtained from Ref. 2. From the data presented there in graph and tabular form the following relationships were arrived at with f/a representing fuel/air ratio and T temperature (°R).

$$R = 53.34 + 7.05 (f/a) \qquad \left[\frac{ft \cdot lb}{lb \cdot °R}\right] \qquad (1)$$

$$C_p = .22626 + .226\,(f/a) + [.0282 - .0219(f/a)]\frac{T}{1000} + [-.0007 + .1581(f/a)]\left(\frac{T}{1000}\right)^2 - [.0042 + .0354(f/a)]\left(\frac{T}{1000}\right)^3 \quad \left[\frac{BTU}{lb\,^\circ R}\right] \quad (2)$$

$$\gamma = \frac{C_p}{C_p - R/778.16}$$

The calculations through the engine will follow the station number nomenclature depicted in Fig. 2.

3.1 DIFFUSER

The biggest assumption in the diffuser calculations is the value or function of ζ (pressure recovery factor) over the Mach range. The Aircraft Industries Association (AIA) has adopted an expression for supersonic ram recovery in a diffuser, (Ref. 1, pg. 137) which was used in these calculations. This curve closely approximates the values presented in Ref. 3, pg. 25, for a 3 shock inlet over the Mach range being considered. As is emphasized in Ref. 1, the penalties incurred in pressure loss for a simple normal shock inlet preclude its use above Mach numbers of approximately 1.5. Above this speed the spike type inlet must be used which results in lower losses by spreading the pressure rise throughout two or more shocks. The reason for the lower losses in an inlet of this type is that the losses across a series of weak shocks are less than the losses across one or several strong shocks. In the 3-shock inlet mentioned, the flow would be compressed through two oblique shocks caused by varying the flow deflection angle of the inlet spike and then through the normal shock occurring within the confines of the inlet itself behind which the flow is naturally subsonic.

Therefore the value of ζ_D used at a flight Mach number of 1.0 was .95 and above that the AIA relationship of $\zeta_D = 1.0 - 0.1\,(M_o - 1.0)^{1.5}$ was used.

As is seen from the above expression that at a flight Mach number of 3.0, which was the limiting value used in this study, the pressure loss in a diffuser of this type assumes significant proportions. At this Mach number the pressure loss is approximately 30% or $P_1/P_o \approx .7$. This recovery loss in the inlet has a direct effect on the thrust produced by the engine. At a flight Mach number of 3.0 the thrust produced by the engine with this type of diffuser would be 70% of the thrust for an ideal engine ($\zeta_D = 1.0$). For flight at speeds much in excess of Mach 3.0 the diffuser will probably have to be an internal compression inlet employing variable geometry (Ref. 3, pg. 29).

The calculations performed for the diffuser analysis were:

$$T_1/T_o = 1.0 + \frac{\gamma_D - 1.0}{2} (M_o)^2 \qquad (1\text{-}1)$$

$$P_1/P_o = \zeta_D \frac{P_{o_1}}{P_o} = \zeta_D \left(T_1/T_o\right)^{\gamma_D/(\gamma_D - 1)} \qquad (1\text{-}2)$$

It is seen that T_1 is a function of γ in the diffuser which in turn is a function of the average temperature in the diffuser $(T_o + T_1)/2.0$. It is apparent that an iteration is necessary and for generating the γ value here, as well as in the other sections where the average value is needed rather than a specified inlet or exit value, an iteration process was specified in the computer program. This particular iteration is quite simple and is not time consuming since it converges very rapidly.

3.2 COMPRESSOR

Three values of sea level compression ratio were investigated, namely, 6, 11, and 16. It was felt that this range encompassed the range from the low to the high pressure ratios used by modern engines in the transonic speed region. Compressor efficiency is naturally a function of pressure ratio and compressor efficiencies of 84.0, 82.0, and 80.0% were used with the respective values of $(P_2/P_1)_{SL}$ of 6, 11, and 16.

$T_2 - T_1 = \Delta T_c$ where

$$\Delta T_c = \frac{(C_p)_c}{C_{p_c}} (T_1)_c \left[\left(\frac{P_2}{P_1} \right)_c^{\frac{\gamma_c - 1}{\gamma_c}} - 1 \right] \frac{1}{\eta_c} \left(\frac{N}{N_{ref}} \right)^2$$

or

$$\Delta T_c = \frac{(C_p)_c}{C_{p_c}} (518.4) \left[\left(\frac{P_2}{P_1} \right)_c^{\frac{\gamma_c - 1}{\gamma_c}} - 1 \right] \frac{1}{\eta_c} \left(\frac{N}{N_{ref}} \right)^2 \qquad (2\text{-}1)$$

The referred RPM was taken as 1 throughout, and the calculation of C_{p_c} involved once again an iteration as C_{p_c} is the average specific heat value in the compressor and thus a function of T_2. T_2 then equals $T_1 + \Delta T_c$

and $$\frac{P_2}{P_1} = \left(1 + \frac{\Delta T_c \eta_c}{T_1} \right)^{\gamma_c / \gamma_c - 1} \qquad (2\text{-}2)$$

The value of γ_c used is obtained from equation (3) using the value of C_{p_c} generated in the iterative process of equation (2-1). P_2/P_o is obtained from the value of P_1/P_o and is equal to $(P_2/P_1)(P_1/P_o)$.

3.3 MAIN BURNER

The combustion efficiency in the main burner is known to be a function of burner inlet pressure, temperature, and velocity of the air mass. That is, it is proportional to pressure and temperature and inversely proportional to velocity. However, throughout this study the emphasis was on generalized, non-dimensionalized terms and it is not possible to express the velocity of the air flow internally as an integral value. Combustion efficiency was made therefore a function of altitude only and the values tabulated below were used. These agree generally with the typical values used in Ref. 1, pg. 258.

Altitude ~	S.L.	20,000	40,000	60,000	80,000
λ_{MB} ~	95	95	90	85	80

λ_{MB} is the pressure loss coefficient and was given the value of .05 (P_2) (Ref. 4, pg. 316). λ_{MB} represents the total of the pressure loss without burning, plus the so-called momentum total pressure loss experienced by all fluids in a constant area channel when heat is added as illustrated by the Rayleigh line problem. Present day turbine blading materials limit the maximum permissable turbine inlet temperature to approximately 2000°R. However, it is realized that much work is being done and will be done to develop high temperature materials that will be suitable for turbine blading and can withstand higher inlet temperatures. To explore the possible performance benefits to be obtained from raising this turbine temperature limitation, the turbine inlet temperature T_3, was in addition to 2000°, assigned values of 2500 and 3000°R.

The fuel used in the calculations was assumed to have a heating value of 18,550 BTU/lb which is fairly standard for hydrocarbon fuels. Thus

$$\left(\frac{f}{a}\right)_{MB} = \frac{T_3 - \frac{C_{p_2}}{C_{p_3}} T_2}{\frac{(18550)\eta_{MB}}{C_{p_3}} - T_3} \qquad (3\text{-}1)$$

for any specified temperature T_3.

The specific heat capacity at station 3 (C_{p_3}) is now a function of the fuel/air ratio as shown in Eq. (2), and hence an iteration is necessary to obtain the correct value of C_{p_3} and in turn the fuel/air ratio in the main burner.

The pressure ratio P_3/P_o is a function of the pressure loss coefficient in the main burner and is expressed by

$$P_3/P_o = P_2/P_o\,(1 - \lambda_{MB}) = P_2/P_o\,(.95)$$

since λ_{MB} was assumed constant and equal to .05.

3.4 MAIN TURBINE

The efficiency of the main turbine was assumed as 87% throughout the range of calculations. Since the main turbine drives the compressor the turbine output must equal the compressor input and the temperature drop across the main turbine is

$$\Delta T_{MT} = \frac{C_{pc}\ \Delta T_c}{C_{p_{MT}}\ (1 + (f/\ldots)_{MT} - b)} \qquad (4\text{-}1)$$

The factor b represents the ratio of bleed air necessary for accessory drive, cabin pressurization, etc., to total air mass flow through the main engine (lb air/lb air). As the air mass flow has a wide range, b will not be considered constant but is taken as a function of flight Mach number and the ambient pressure. At speeds in excess of Mach 1, the air necessary for cabin pressurization (a complete change every 3 minutes) for a transport size aircraft was considered with respect to the air flow through an engine. This was determined to be approximately 1-2% of the total air flow. Power for accessory drive is hard to estimate; hence a value for b of .05 was assumed for the engine at 40,000 feet at Mach 1. As the per-cent bleed at other conditions is a function of altitude, the following relationship for b was assumed to hold. In this expression bleed air is inversely proportional to the mass flow rate through the engine.

$$b = \frac{\ldots\ T_{\ldots}}{P_{\ldots}\ (M_{\ldots})} \qquad (4\text{-}2)$$

Once ΔT_{MT} is determined from the iteration of Eq. 4-1 with $C_{p_{MT}}$, then

$$T_4 = T_3 - \Delta T_{MT}$$

and

$$P_4/P_3 = \left(1 - \frac{1}{T_{\ldots}\ \eta_{MT}}\right)^{\ldots\ (\ldots - 1)}$$

$$P_t/P_2 = (P_4/\ldots)(P_{\ldots})$$

3.5 FAN TURBINE

As shown in Fig. 2 the fan turbine was considered as entirely separate from the main turbine of the engine. Hence it is a free wheeling turbine which drives the compressor fan in the by-pass section.

The turbofan configuration considered in this study is a so-called aft fan. In such an arrangement, the fan is driven by its own turbine stage located aft of the main turbine as shown schematically in Fig. 2. There are also in use today front fan engines as exemplified by the Pratt and Whitney JT3D turbofan. In this type engine, a twin spool compressor is used whose forward section has a greater diameter to compress the air flow before a portion of it is bypassed. As might be expected, both systems have their merits. Proponents of the front fan cite the fact that a conventional single air inlet is used and that with the mechanically coupled arrangement, it is possible to use multiple stages to obtain the highest fan efficiency and greatest freedom of cycle choice. General Electric with their CJ805-23 aft fan engine cites the advantages of simplicity of design and operation and the fact that coupling an aft fan arrangement to an existing turbojet engine does not effect the mechanical configuration or thermodynamic cycle of the basic jet. Both designs have particular merits but in the interest of simplicity an aft fan engine was chosen for the cycle computations.

The energy input to the fan can be expressed similarly as the energy input of the compressor. The calculation for the temperature difference across the fan is thus similar to Eq. 2-1.

$$\Delta T_F = \frac{.240 \times 518.4}{c_{p_F}} \left[\left(P_4/P_0 \right)_{SL}^{.2857} - 1.0 \right] \frac{1}{\eta_F} \qquad (5\text{-}1)$$

A fan efficiency of 87% was assumed throughout.

Since the energy output of the fan turbine must equal the energy input of the fan, the temperature difference across the fan turbine can be calculated for a given by-pass ratio μ by

$$\Delta T_{FT} = \mu \frac{\Delta T_F}{\left(1 + (\dot{W}_f/\dot{W})_{MB} - b\right)} \frac{c_{p_F}}{c_{p_{FT}}} \qquad (5\text{-}2)$$

T5 is then equal to T4 - ΔT_{FT} and the pressure ratio across the fan turbine is

$$P_5/P_4 = \left(1 - \frac{\Delta T_{FT}}{T_4\, \eta_{FT}}\right)^{\gamma_{FT}/\gamma_{FT}-1}$$

A fan turbine efficiency of 87% was used throughout the calculations. The pressure ratio at station 5 to ambient is

$$P_5/P_2 = (P_5/P_4)(P_4/P_2)$$

3.6 AFTERBURNER

The afterburner temperatures assigned in the main program were T6 = T5 (no afterburning), 2500°, and 3000°R. To examine the effects of dissociation if reheat temperatures could be raised above 3000°, the range was expanded for one computer program to 5000°R. The assumptions made in this calculation are contained in the section, Additional Computer Calculations. It is realized however, that the materials available today limit tail pipe temperatures to the vicinity of 3000°R. The fuel/air ratio in the afterburner was determined by:

$$(f/a)_{AB} = \frac{(1 + (f/a)_{MB} - b)(T_6 - \frac{C_{P_2}}{C_{P_6}} T_2)}{(18{,}550)\, \eta_{AB}/C_{P_6} - T_6} \qquad (6\text{-}1)$$

The afterburner efficiency used is the same as the efficiency of the main burner. This relationship again requires an iteration, as C_{P_6} is a function also of $(f/a)_{AB}$ calculated in Eq. 6-1.

The pressure loss coefficient λ_{AB} in the afterburner was assumed as .05. Hence,

$$P_6/P_2 = \frac{P_5}{P_2}(1 - \lambda_{AB}) = .95\, P_5/P_2$$

3.7 MAIN NOZZLE

In the nozzle the energy available in the exhaust gases is at least partly converted into kinetic energy to produce thrust. Efficiency is all important in a nozzle and a polytropic efficiency of 94% was used. The nozzle was assumed to be of the convergent type although later in this report the merits of the convergent-divergent nozzle will be discussed. The two air streams are assumed to be still divided at this point and hence there are two sections for the nozzle calculations, one for the main nozzle and one for the fan by-pass nozzle. Knowing the flow conditions at station 6, it then remains to calculate the velocity and static pressure in order to determine the thrust obtained. The polytropic exponent n is determined from $n = \frac{\gamma}{\gamma(1-\eta_{pn})+\eta_{pn}}$ where η_{pn} represents the afore-mentioned efficiency.

The basic thrust equation is

$$T_n = \frac{\dot{m}}{g}\left(1 + (f/A)_{mix} + (f/A)_{ab} - b\right)V_7 + A_7(P_7 - P_0) - \frac{\dot{m}}{g}V_0 \qquad (7\text{-}1)$$

The velocity term is determined from

$$\frac{V_7^2}{2g} = C_{p_n}(T_6 - T_7) = C_{p_n} T_6 \left(1 - (P_7/P_6)^{n/n-1}\right)$$

Non-dimensionalizing, this becomes

$$\frac{V_7}{\sqrt{\gamma_6 R T_6}} = \sqrt{\frac{2}{\gamma_6 - 1}\,\frac{T_6}{T_0}\left[1 - (P/P)^{n/n-1}\right]} \qquad (7\text{-}2)$$

It thus becomes necessary to determine the actual static pressure at the throat (7) by calculating the critical pressure ratio at the given flow conditions and comparing it with the calculated pressure ratio P6/P0. The critical pressure ratio for a polytropic expansion is given by

$$PR_{CRIT} = \left(\frac{2}{n+1}\right)^{\frac{n}{n-1}} = P_7/P_6$$

The velocity term $V_1/\sqrt{gRT_c}$ (which was given the designation C7 in the computer calculations) is thus expressed by

$$C7 = \sqrt{\frac{2\gamma_N}{\gamma_N - 1}\frac{T_1}{T_c}\left[1 - \left(P_1/P_c\right)^{\frac{n-1}{n}}\right]}$$

for sub-critical conditions, and by

$$C7 = \sqrt{\frac{2\gamma_N}{\gamma_N - 1}\frac{T_c}{T_c}\left(\frac{n-1}{n+1}\right)}$$

for critical and super-critical flows. Mass flow per unit nozzle discharge area is given by

$$\frac{\dot{m}_1}{A_1} = \left\{\frac{2g\,\gamma_N P_c^2}{R(\gamma_N - 1)T_c}\left[\left(\frac{P_1}{P_c}\right)^{2/n} - \left(\frac{P_1}{P_c}\right)^{\frac{n+1}{n}}\right]\right\}^{1/2} \qquad (7\text{-}3)$$

Non-dimensionalizing, this expression becomes $\frac{\dot{m}}{A_1}\sqrt{\frac{T_c}{P_c}}\sqrt{R/g}$

and giving this term the designation CA for the calculations, the equation becomes

$$CA = \frac{P_1}{P_c}\sqrt{\frac{T_c}{T_c}\frac{\gamma_N}{\gamma_N - 1}\left[\left(\frac{P_1}{P_c}\right)^{2/n} - \left(\frac{P_2}{P_c}\right)^{\frac{n+1}{n}}\right]}$$

for sub-critical flow, and since $\frac{P_1}{P_c} = \left(\frac{2}{n+1}\right)^{\frac{n}{n-1}}$ for critical pressure ratios, the term becomes

$$CA = \frac{P_c}{P_1}\left(\frac{2}{n+1}\right)^{\frac{1}{n-1}}\sqrt{\frac{T_c}{T_c}\frac{2\gamma_N}{\gamma_N - 1}\left(\frac{n-1}{n+1}\right)}$$

for supercritical flow conditions. The thrust equation (Eq. 7-1) in non-dimensionalized form thus becomes

$$\frac{T_n}{\dot{m}}\sqrt{\frac{g}{RT_t}} = THS = \left(1 + (f/a)_{MB} + (f/a)_{AB} - b\right) C_7 + \left(1 + (f/a)_{MB} + (f/a)_{AB} - b\right)\left(\frac{P_7}{P_t} - 1\right)/CA - \frac{V_\infty}{g}\sqrt{\frac{g}{RT_t}}$$

As p_7, the nozzle exit pressure, equals the static ambient pressure at sub-critical conditions the expression for the thrust non-dimensionalized and designated THS in the program is given by

$$\frac{T_n}{\dot{m}}\sqrt{\frac{g}{RT_t}} = THS = \left(1 + (f/a)_{MB} + (f/a)_{AB} - b\right) C_7 - M_\infty\sqrt{\theta} \qquad (7\text{-}4a)$$

for sub-critical flow, and

$$THS = \left(1 + (f/a)_{MB} + (f/a)_{AB} - b\right) C_7 - \left(1 + (f/a)_{MB} + (f/a)_{AB} - b\right)\left(P_7/P_t - 1\right)/CA - M_\infty\sqrt{\theta} \qquad (7\text{-}4b)$$

for supercritical flow.

Since it is more descriptive to define specific thrust in units of lb. thrust per lb. air/sec. in lieu of the completely dimensionless term THS of equations 7-4a and 7-4b, these terms were multiplied by the term $\sqrt{\frac{RT_t}{g}}$. Therefore, the term TS1 in the results of the enclosed appendix denotes the specific thrust generated in the main engine and has the units lb. thrust/lb.air/sec.

The specific fuel consumption is a measure of the economy of the engine and is defined by lbs of fuel burned per lb. of thrust per hour. The specific fuel consumption, SF1, in the main engine is equal to

$$SF1 = \left[(f/a)_{MB} + (f/a)_{AB}\right] 3600 / TS1$$

3.8 FAN

As was mentioned previously, the by-pass diffuser is considered the equal of the main engine diffuser and hence all flow conditions at station 8 were considered identical to those at station 1. The temperature increase across the fan was likewise obtained similarly to that of the compressor (Eq. 2-1), namely, by expressing the temperature rise as a function of the designated fan pressure ratio at sea level. This calculation was performed in the fan turbine section by Eq. 5-1. For this study, sea level values of the fan pressure ratio of 1.3, 1.5, and 1.7 were used as they encompass the range of values used today in the turbofans. These pressure ratios correspond to approximate temperature rises of 40, 70, and 100°F, respectively. An efficiency of 87% was assumed for the fan throughout its range of values.

The temperature at station 9 aft of the fan is then given by

$$T_9 = T_8 + \Delta T_F \qquad (8\text{-}1)$$

and the pressure ratio across the fan by:

$$\frac{P_9}{P_8} = \frac{P_9}{P_8} = \left(1 + \frac{\Delta T_F \eta_F}{T_8}\right)^{\frac{\gamma_8}{\gamma_8 - 1}}$$

3.9 FAN AFTERBURNER

The fan afterburner temperature T_{10} was assigned values of 2000°, 2500°, and 3000°R for the calculations. Calculations were also made with no fan afterburning, that is $T_{10} = T_9$, but as might be expected, between Mach 1 and 2 the slight thrust present at the lower Mach number turns into a negative thrust or drag as speed is increased. Accordingly, in the results tabulated in section D of the Appendix the values assigned to T_{10} were the previously mentioned ones. The fuel/air ratio is calculated similarly to that in the main engine burner, Eq. 6-1, and hence

$$\left(\frac{f}{a}\right)_{FAB} = \left(T_{10} - \frac{C_{p_9} T_9}{C_{p_{10}}}\right) \Big/ \left(\frac{h_{PR}}{C_{p_{10}}}\Big|_{FAB} - T_{10}\right) \qquad (9\text{-}1)$$

The burner efficiency was assumed equal to the main burner efficiency (a function of altitude), and the pressure loss coefficient λ also equal to .05 thus

$$P_{t_6}/P_2 = P_3/P_2 \left(1 - \lambda_{FAB}\right) = .95\, P_3/P_2 \qquad (9\text{-}2)$$

3.10 FAN NOZZLE

The calculations necessary for determining the thrust of the fan nozzle and the specific fuel consumption are identical to those previously described for the main nozzle. Thus it is first necessary to determine whether critical conditions exist in the convergent nozzle for the pressure and temperature present at station 10. The terms C7 and CA defined in the Main Nozzle section are then calculated and the non-dimensionalized thrust in the fan by-pass (THFS) is given by

$$THFS = \left(1 + (f/a)_{FAB}\right) C7 - M_0 \sqrt{\delta_0} \qquad (10\text{-}1)$$

for sub-critical nozzle flow, and

$$THFS = \left(1 + (f/a)_{FAB}\right) C7 + \left(1 + (f/a)_{FAB}\right)\left(P_{t_7}/P_2 - 1\right) CA - M_0 \sqrt{\delta_0} \qquad (10\text{-}2)$$

for supercritical flow.

TS2 (lbs. thrust/ lb. air/sec.) and SF2 (lbs. fuel/lb. thrust/hour) are obtained similarly to the corresponding terms for the main nozzle.

3.11 MAIN COMPUTER PROGRAM OUTLINE

On the following pages the flow chart for the computer program is outlined. Although a table of symbols used in the programming is included in section A of the Appendix, a similar table which converts the various symbols used in the analysis is contained in the Table of Symbols found on page 2.

For convenience in programming the problem, all of the calculations for a particular section of the engine are included in a separate subroutine. The subroutine designations for the various sections are as follows:

DIFU - Diffuser
COMP - Compressor
MB - Main burner
MT - Main turbine
FT - Fan turbine
AB - Afterburner
NM - Main nozzle
FAN - Fan
FAB - Fan afterburner
NFAN - Fan by-pass nozzle

PROGRAM FLOW CHART

MAIN PROGRAM

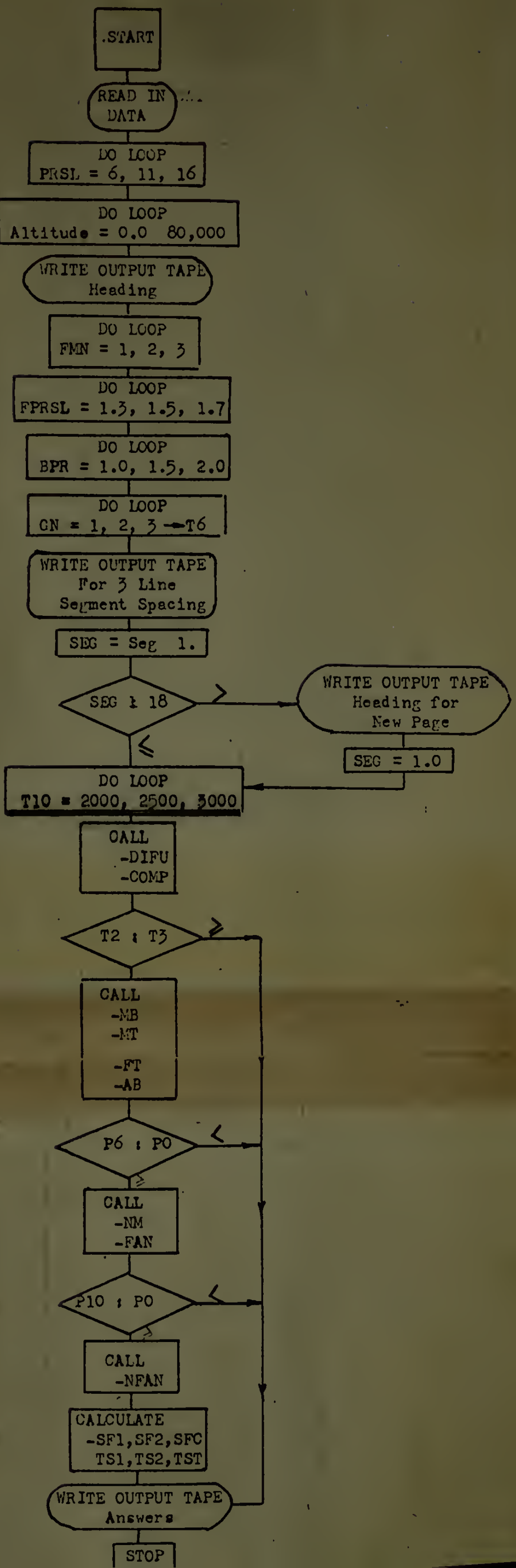

FUNCTION CP (Fuel/Air Ratio & Temp)

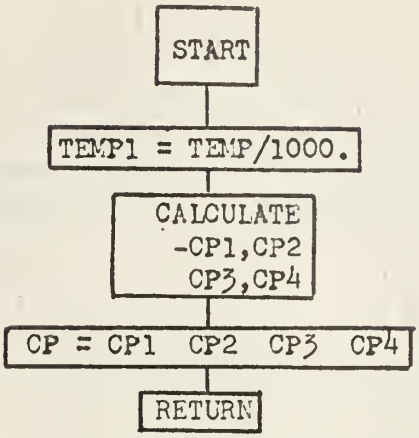

FUNCTION GAM (Fuel/Air Ratio & Temp)

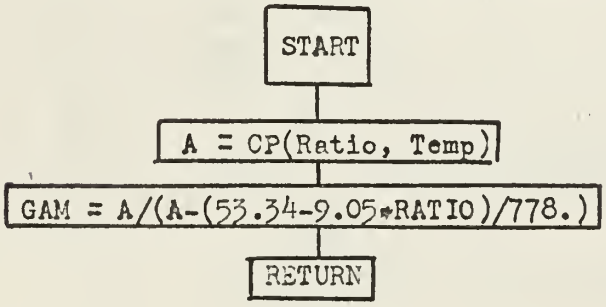

FUNCTION EN (Gamma & Efficiency)

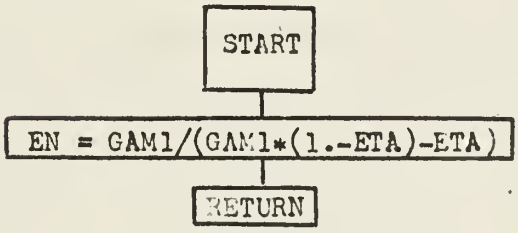

FUNCTION TA (Altitude)

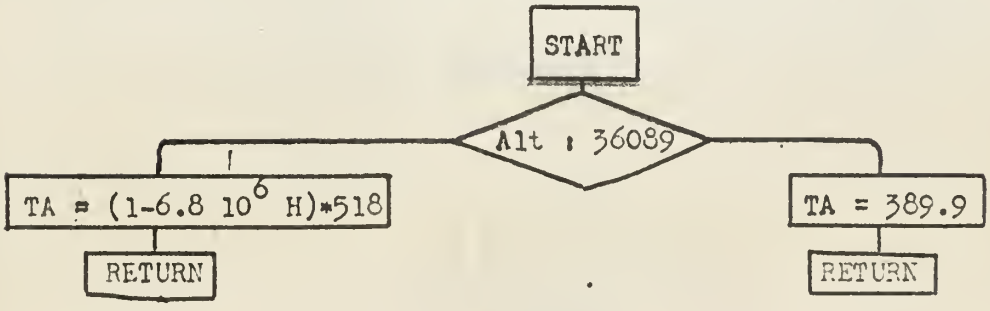

FUNCTION PA (Altitude)

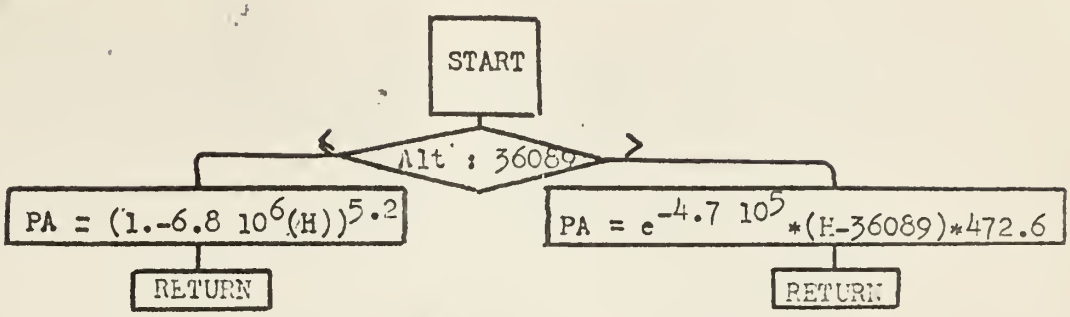

SUBROUTINE DIFU

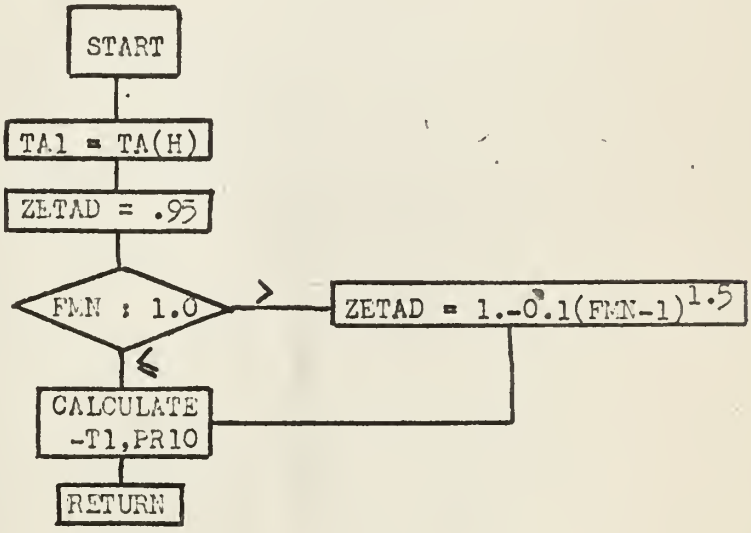

SUBROUTINE COMP

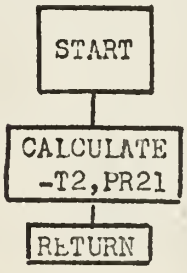

SUBROUTINE MB

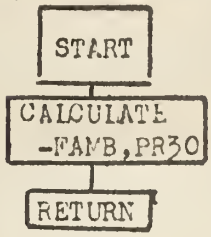

SUBROUTINE FT

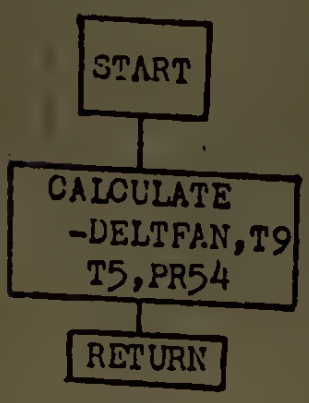

SUBROUTINE AB

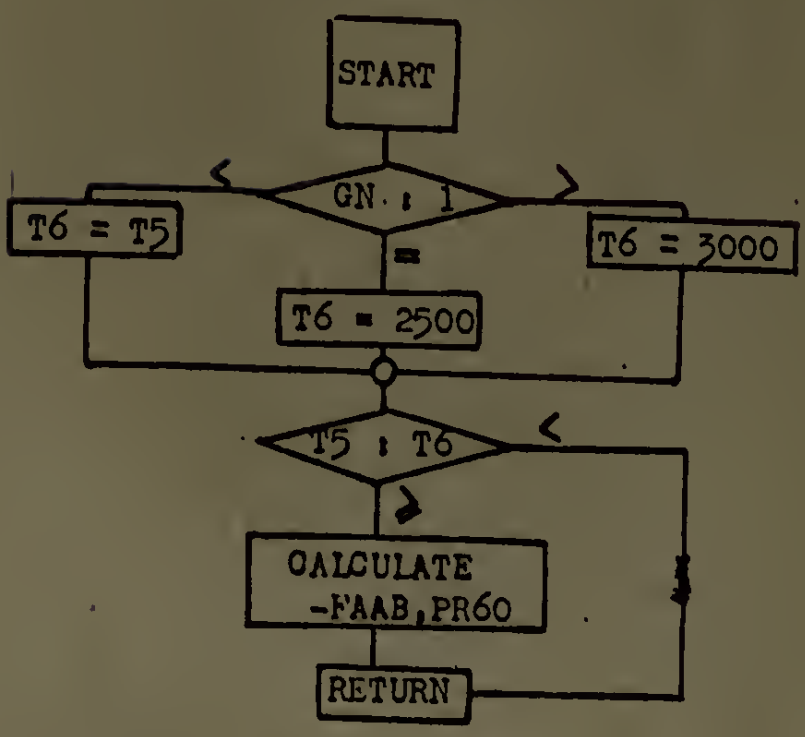

SUBROUTINE NM

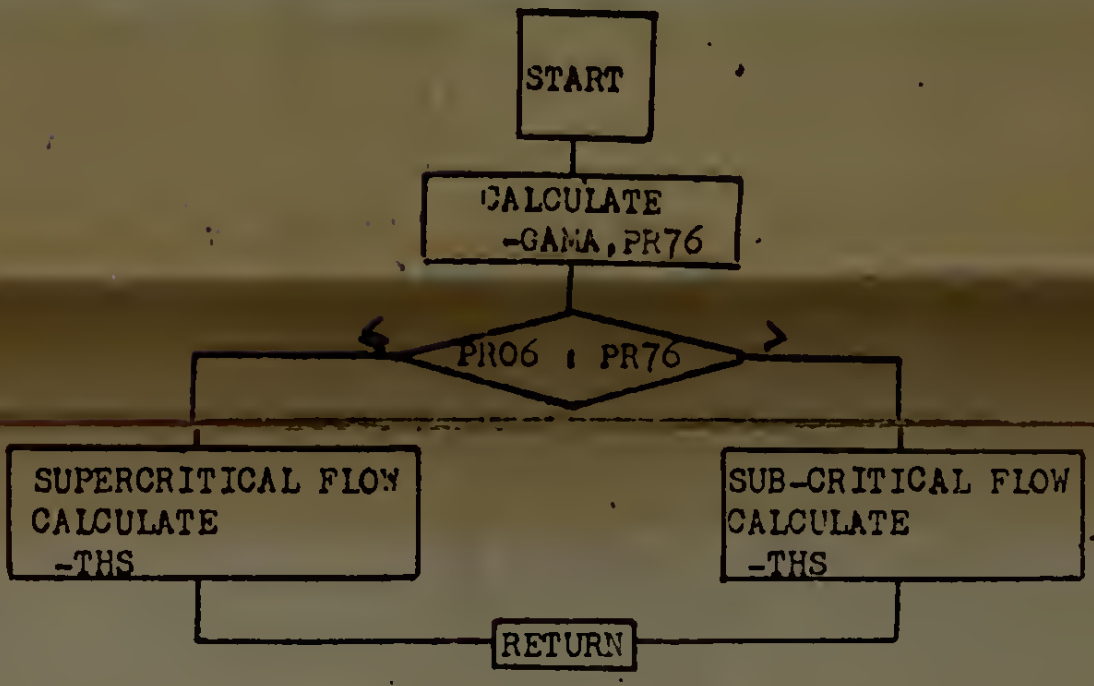

SUBROUTINE FAN

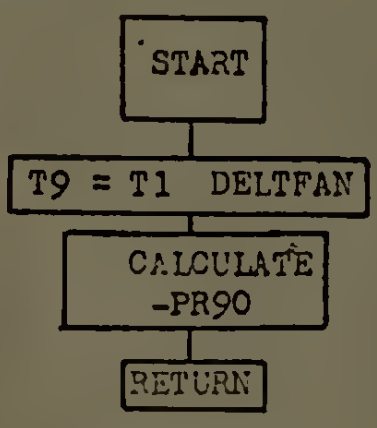

SUBROUTINE FAB

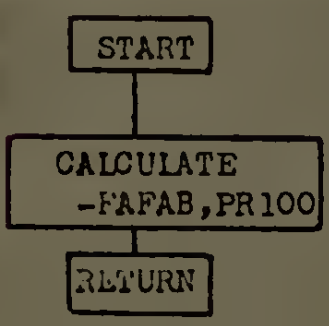

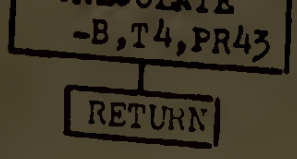

SUBROUTINE FT

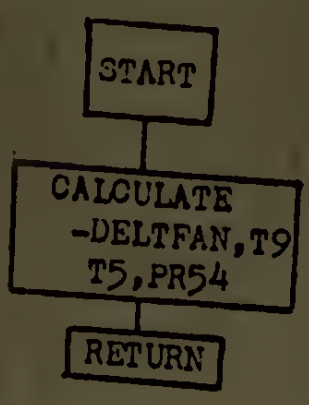

SUBROUTINE AB

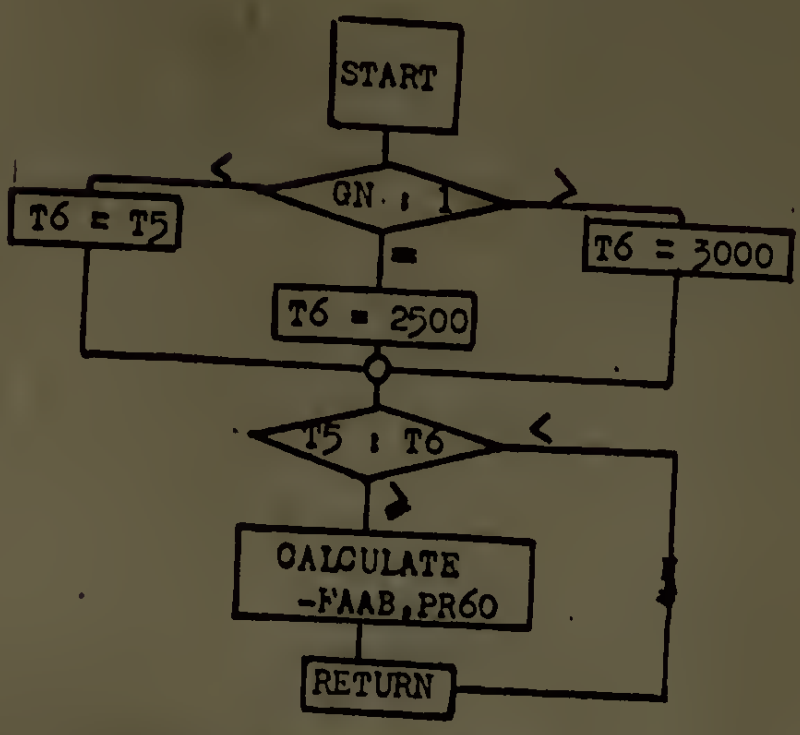

SUBROUTINE NM

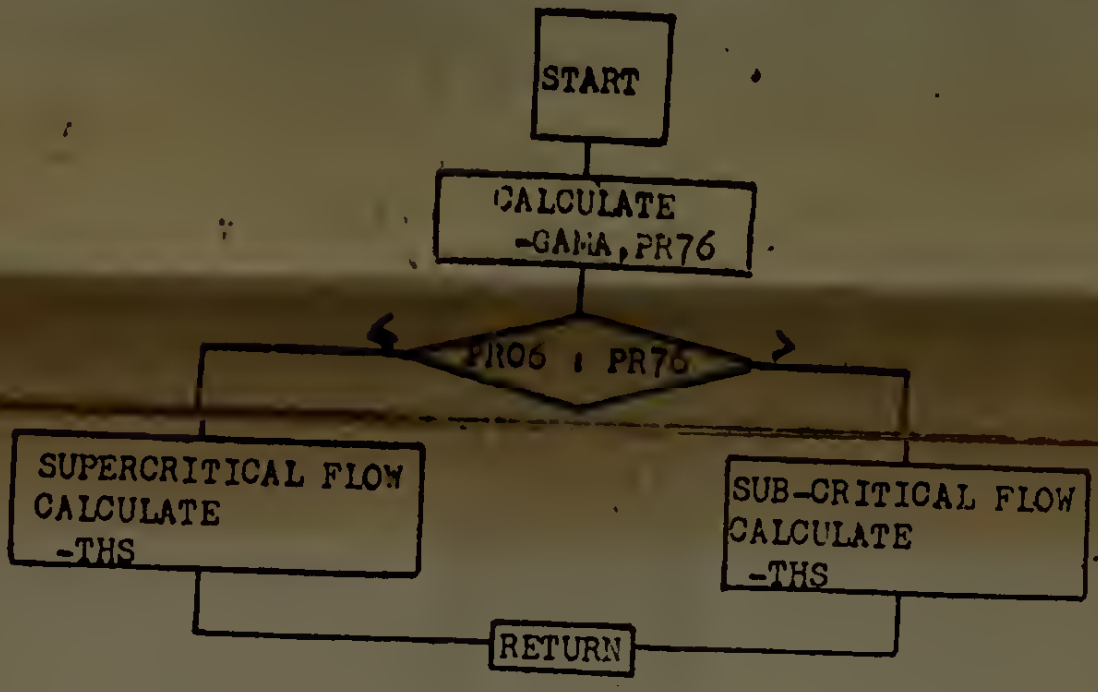

SUBROUTINE FAN

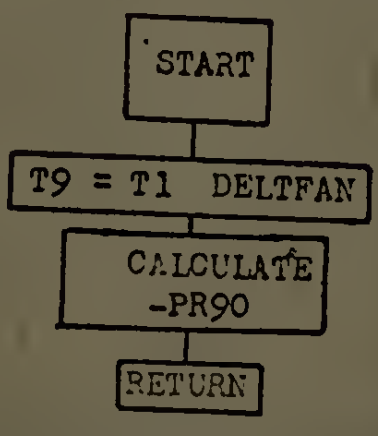

SUBROUTINE FAB

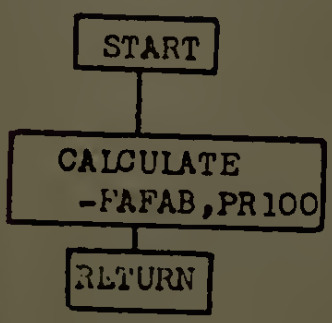

3.12 ADDITIONAL COMPUTER CALCULATIONS

In addition to the main program as outlined other similar programs to investigate the merits of related type engines were run. With the program this was quite simple. By setting the by-pass ratio equal to zero and the fan pressure ratio equal to 1.0, a straight jet engine is simulated. The results contained in section C of the Appendix were generated in this manner. Further, to investigate the performance of a pure by-pass engine with afterburning in the by-pass section, in other words a straight jet enclosed by a ram jet, it was merely necessary to set the fan pressure ratio to 1.0. This in effect eliminates the fan, and the by-pass afterburner temperature was varied along with the by-pass ratio to fully investigate the possibilities of such a type engine.

In addition to this, a program was run to investigate the effects of afterburning at temperatures in excess of $3000^{\circ}R$. Above 3000° dissociation becomes a factor and thus specific heat becomes not only a function of temperature and fuel/air ratio as before, but also of pressure. Such an analysis becomes purely theoretical since one must make assumptions as to just when dissociation and in turn recombination take place in the engine. These reactions are not instantaneous but are functions of time and hence assumptions must be made as to the state of equilibrium of the hot exhaust gases as they pass through the nozzle. For this study, a frozen equilibrium was assumed. This means that the equilibrium products of the dissociation reactions present in the afterburner combustion, for that particular temperature and pressure are maintained for the flow through the nozzle. Afterburner temperatures (T6) of 3500, 4000, 4500, and $5000^{\circ}R$ were used in this calculation at altitudes of 50,000 and 70,000 feet. With the energies of dissociation included in the calculations it was necessary to alter the expression for the mean specific heat of the combustion gases. For this calculation, the thermodynamic values listed in Ref. 4 for the combustion gases were used for each temperature and pressure, with an iteration to calculate the correct specific heat capacity for each generated value of fuel/air ratio.

From the results obtained for the calculations of the straight jet engine, which are contained in section C of the Appendix, it is seen by comparing P7/P6 to Po/P6, that the nozzle flows are all supercritical and

as Mach number is increased the pressure ratio in the nozzle becomes quite large. Thus the performance of a convergent-divergent nozzle which can take advantage of these large pressure ratios and exhaust the gases at supersonic velocities was examined. To investigate the relative merits of a convergent and a convergent-divergent nozzle at these supercritical pressure ratios, the basic thrust equation for gross thrust (neglecting ram drag) was non-dimensionalized to

$$Th/P_2 A_7 = \frac{\dot{m} V_7}{g P_2 A_7} + \left(\frac{P_7}{P_2} - \frac{P_2}{P_2}\right) \qquad (11)$$

For supercritical conditions in the convergent nozzle the critical Mach number for flow with friction is equal to

$$M_{CRIT} = \sqrt{\frac{\gamma - 1}{\gamma + 1}}$$

The velocity at the nozzle exit, V_7 is equal to

$$V_7 = a_7 M_{CRIT} = a_7 \left(\frac{a_6}{a_6}\right) M_{CRIT} = a_6 \left(\frac{T_7}{T_6}\right)^{1/2} M_{CRIT} = a_6 \left(\frac{2}{\gamma+1}\right)^{1/2}$$

The mass flow rate of the exhaust gases $\dot{m}$ is equal to $\rho_7 A_7 V_7$, and the critical pressure ratio P6/Po is given by $\left(\frac{\gamma+1}{2}\right)^{\gamma/\gamma-1}$. The non-dimensionalized thrust for the convergent nozzle is

$$Th/P_2 A_7 = \left(\frac{2}{\gamma+1}\right)^{\frac{1}{\gamma-1}} \left[1 + \gamma\left(\frac{\gamma-1}{\gamma+1}\right)\right] - \frac{P_2}{P_2} \qquad (12)$$

In a fully expanded convergent-divergent nozzle, the nozzle exhaust pressure is equal to the ambient pressure and the differential pressure is zero, thus Eq. 11 reduces to

$$Th/P_2 A_7 = \left(\frac{\dot{m}}{g P_2 A_7}\right) V_7 \qquad (13)$$

The only term different here in comparison to the first term of equation (11) is the exit velocity V_7. For the fully expanded nozzle the velocity head is represented by:

$$\frac{V_7^2}{2gJ} = C_p (T_6 - T_7) = \frac{\gamma}{\gamma-1} \frac{R}{J} T_6 \left[1 - \left(\frac{P_7}{P_6}\right)^{\frac{\gamma-1}{\gamma}}\right]$$

or:

$$V_7 = a_7 \sqrt{\frac{2}{\gamma - 1}\left[1 - \left(\frac{P_7}{P_0}\right)^{\frac{\gamma-1}{\gamma}}\right]}$$

Substituting this value for V_7 in (13) the non-dimensionalized gross thrust for a convergent-divergent nozzle becomes

$$\frac{Th}{P_2 A_7} = S^* \left(\frac{2}{\gamma+1}\right)^{\frac{\gamma+1}{2(\gamma-1)}} \sqrt{\frac{\gamma+1}{S^*-1}\left(\frac{2}{S^*-1}\right)\left[1 - \left(\frac{P_7}{P_0}\right)^{\frac{\gamma-1}{\gamma}}\right]}$$

These two relationships were compared at varying supercritical pressure ratios with the tabulated results contained in Appendix E. To illustrate the importance of nozzle efficiency on thrust, the convergent nozzle polytropic efficiency was assumed as 95% and the convergent-divergent nozzle efficiency was varied from 85 to 95%. The efficiencies of the convergent-divergent nozzle are smaller since at supercritical pressure ratios the flow passages for the expansion to ambient pressure will be longer than in the converging nozzle.

4. RESULTS

The results of the main computer calculations are in the Appendix. (Because of the magnitude of computer output involved, the results were placed in a separate Appendix enclosure.) The results for the straight jet engine are given in section C, and for the turbofan with main and by-pass afterburning in section D. Because of the length of the tabulated data, section D was further divided into three sections corresponding to the compressor pressure ratio values of 6, 11, and 16. One of the main conclusions of the investigation which is shown graphically in Fig. 3 and 4, is the inferior performance of the high compression turbojet in these high speed regions. Although a high compression ratio is desirable in subsonic engines, (the J-57 has a compressor rating of 16.0), it is a definite liability at high altitude and high Mach number flight. That this is in fact true is shown by comparing PRSL values of 6 and 16 at 70,000 feet and a Mach number of 3 from Appendix B.

	PRSL = 6.0	PRSL = 16.0
η_c	.84	.80
P_2/P_1	2.7	5.19
ΔTc	390^o	730^o
ΔT_{MT}	386^o	762^o

The actual pressure ratio delivered by the two compressors at this Mach number should be noted. Whereas the sea level values are in the ratio of 18:6 or 3 to 1, it is seen that the ratio now has diminished to 5.19:2.7 or 1.92 to 1.

Futhermore with the pressure ratio across the turbine expressed by $\frac{P_4}{P_3} = \left(1 - \frac{\Delta T_{MT}}{T_3 \eta_{MT}}\right)^{\frac{\gamma}{\gamma-1}}$ it is seen that the larger compressor requires a much larger relative temperature difference across the driving turbine and the pressure drop in turn is also considerably greater. Using a value for γ in the turbine of 1.33 the pressure ratio across the turbine is .348 for PRSL = 6.0 and .073 for PRSL = 16.0.

With the pressure drops in the burner sections approximately the same, P_6/P_o is approximated by $\frac{P_1}{P_o}\ \frac{P_2}{P_1}\ \frac{P_4}{P_3}$, and thus the pressure upstream of the nozzle for the lower compressor pressure ratio is actually higher than for the high compression engine. This lower pressure results in a lower specific thrust for the high compressor ratio engine. This thrust comparison is reflected in all of the calculations for the turbojet and also for the turbofan. For this reason most of the comparitive performance graphs are drawn for a PRSL 6.0 engine since it represents the highest performance engine.

Since any projected supersonic aircraft, transport or otherwise, would still spend a fair percentage of its flight time in the transonic speed region below 50,000 feet while climbing out or descending, it is well to look at the turbofan-turbojet comparison in this flight region. From Fig. 4 and 5 it is seen that the best turbofan performance is achieved by the smaller by-pass ratio of 1.0 and the higher fan pressure ratio of 1.7. In comparison to the turbojet in this region though, it is seen in Fig. 5 that the turbojet enjoys a performance advantage of roughly 5-10% throughout the altitude range of 0-50,000 feet.

Mach 1 flight results will not be examined here for altitudes above 50,000 feet since it is not realistic to investigate flight performance for conventional aircraft at speeds in this region that are subsonic. Since indicated air speed is equal to $\sqrt{2q/\rho}$ it is seen that to maintain an indicated flight speed of 150 Kts requires a dynamic pressure q of 74 lbs/ft^2. A dynamic pressure head of 74 lbs/ft^2 at 50,000 feet corresponds to a flight Mach number of .7 and is supersonic at 70,000 feet. As 150 Kts represents a landing pattern speed for todays high performance aircraft it was not considered worthwhile to study the Mach 1 results beyond 50,000 feet.

At 50,000 feet the performance for the turbojet and the turbofan was investigated throughout the chosen Mach number range. It is seen from Fig. 6 that the performance of the turbofan is essentially not dependent on by-pass ratios at Mach numbers of 2 and greater. Further it is seen

that at this altitude the afterburning turbofan begins to show a noticeable performance advantage over the turbojet above Mach 2.0.

In Fig. 7, the Mach 2 flight envelope was investigated from 40,000 to 70,000 at a by-pass ratio of 1.0 with varying fan pressure ratios. It is seen that the turbofan engine is essentially independent of the fan pressure ratio as it was of the by-pass ratios at the higher Mach numbers. It is also evident from the figure that for a constant Mach number of 2, the turbofan begins to show an increasing performance advantage above 55-60,000 feet.

Figure 8 illustrates the performance of the turbofan at varying by-pass ratios over the same flight envelope examined in Fig. 7. Once again it is seen that performance is essentially independent of by-pass ratio up to an altitude of approximately 70,000 feet where the by-pass ratio 2.0 engine has a slightly higher specific thrust and lower specific fuel consumption. This comparison is also shown in a slightly different manner by the bar graph in Fig. 9. The effect of varying the compressor ratio is illustrated in Fig. 10 with the same results as mentioned previously for the turbojet engine; that is, performance is inversely proportional to the compressor pressure ratio with a substantial difference between the compressor pressure ratios of 11 and 16.

In the Mach 3 flight region the afterburning turbofan shows a substantial performance advantage over the turbojet. Figure 11 compares the turbofan with varying fan pressure ratios to the straight jet. It is seen that performance is again independent of the fan pressure ratio, and that the performance advantage of the turbofan increases uniformly with altitude. At this Mach number the by-pass ratio makes a noticeable difference as shown in Fig. 12. The higher by-pass ratio value of 2.0 shows the highest specific thrust and consequently lowest fuel consumption with a performance advantage of 26% in comparison to the straight turbojet at 80,000 feet.

With this demonstrated performance of the high by-pass ratio turbofan in the high altitude Mach 3 flight area, it is of interest to examine next where the combination ram-turbojet, ranks performance-wise. In essence this amounts to simply removing the fan and the fan turbine from

the previous program for the turbofan. In Fig. 13, Mach 1 flight is compared with varying by-pass ratios for the ram-turbojet to the previously calculated performance of a turbofan with a fan pressure ratio of 1.7 and a by-pass ratio of 1.0. The engines were compared at this Mach number in the same mode of operation, that is, with no afterburning in the main jet and with 2000°R reheat in the by-pass section. It is evident that the turbofan is markedly superior to the ram by-pass engine since the specific thrust of the turbofan is approximately 25% better than that of the ram engine over the entire altitude range. The ram engine is similar to the turbofan in this flight area in that the best performance is achieved by the engine with the smaller by-pass ratio.

As speed and altitude are increased to the Mach 2 and 40-70,000 feet regime, it is seen that the ram engine and the by-pass fan engine are much more closely matched in performance. At this Mach number the turbofan still enjoys a slight performance advantage of approximately 5% which diminishes with increasing altitude. As Mach number is increased to 3, (see Fig. 15), the ram engine is almost identical in performance to the turbofan. As was found with the turbofan at Mach 3, the highest performance is achieved with the by-pass ratio of 2.0. The figure shows a slight performance advantage for the ram engine at higher by-pass ratios in comparison to the turbofan. However, the turbofan illustrated here, is an engine with a by-pass ratio of 1.0, and at the higher by-pass ratios (see Fig. 12) it is seen that the performance of the two engines (with similar configurations) is the same. Therefore, as the flight Mach number is increased to 3.0, the performance advantage of the turbofan in comparison to the ram-turbojet continually decreases and at speeds in excess of Mach 3 an extrapolation of the data would indicate superior performance for the combination ram-turbojet in comparison to the turbofan.

In addition to the results obtained from the main program outlined above, it is interesting to investigate the engine performance possibilities if the present temperature limits in gas turbine engines could be raised. The turbojet, turbofan, and ram-turbojet engines were compared assuming a turbine inlet temperature of 2000°R and afterburning temperature limit

of 3000°R. These are the approximate temperature limits imposed by the available materials used in jet engine construction today. Since the work output of a turbine is equal to

it is seen the power developed is directly proportional to turbine inlet temperature. Hence, a direct method of increasing engine performance is by raising this temperature restriction. Much work has been done and will be done on external and internal methods of turbine blade cooling and Fig. 16 shows graphically the advantages to be gained by finding a solution to this restriction. It is seen that in the Mach 2-3 flight envelope from 40 to 80,000 feet that specific thrust increases uniformly with increasing turbine inlet temperatures and at the same time the specific fuel consumption is decreasing. The thrust increases shown are significant and hence increasing the permissable turbine inlet temperature represents one of the most direct methods of increasing the performance of a gas turbine engine.

Also investigated was the effect of raising afterburning temperatures from 3000°R, at 500° intervals, to 5000°R. Above 3000°R the combustion of a hydrocarbon fuel results in dissociation to a degree dependent on temperature, pressure, and fuel/air ratio. The thermodynamic properties of the combustion gases in this area were obtained from Ref. 4. Figures 17 and 18 illustrate how the average specific heat capacity varies as a function of these three variables. By using values of specific heat that include the dissociation effects, the performance parameters of Fig. 19 were obtained. These performance values were obtained by assuming a frozen equilibrium for the gas passing through the nozzle. As is shown, tremendous specific thrusts are obtainable at the price of large fuel comsumptions. At temperatures approaching 5000°R the fuel/air ratio approaches and sometimes exceeds values of three times stoichiometric. At fuel/air ratios of three times stoichiometric and greater, there is a considerable amount of solid carbon in the combustion products and specific heat values for the combustion are not tabulated. Fuel/air ratios of three or greater are represented by broken lines in Fig. 19. The large fuel consumptions shown by the figure assume asymptotic proportions as temperature is increased towards 5000°. This is due to

the energy involved in dissociation which represents unavailable energy as far as creating kinetic energy for thrust is concered.

The non-dimensionalized gross thrust for the convergent and convergent-divergent nozzle comparison is tabulated in Appendix E and also in Fig. 22 for supercritical pressure ratios. Fig. 22 illustrates a comparison where the efficiency of both nozzles was assumed equal to 100%. It is seen from Fig. 22 that even with frictionless flow the convergent-divergent nozzle is not clearly superior to the plain convergent nozzle at all supercritical pressure ratios. The converging-diverging nozzle does not show a definite advantage until pressure ratios of 4 to 5 are reached. The importance of nozzle efficiency is illustrated in the comparison of Fig. 23. The convergent nozzle efficiency was assumed here as 95% and the efficiency of the convergent-divergent nozzle was assumed to have different values ranging from 85-95%. The lower efficiency values for the convergent-divergent nozzle were assumed since the flow would be expanding in the nozzle to discharge at ambient pressure.

It is seen from the figure that with the lower efficiencies, the convergent-divergent nozzle is actually inferior until pressure ratios of approximately 10/1 to 12/1 are reached. Nozzle pressure ratios of this magnitude, 10/1 to 12/1, are obtained at Mach 3 flight but it is seen that up to this point the convergent-divergent nozzle is actually a drawback to engine performance. That this is in fact true is illustrated in Figs. 24, 25, and 26, where the basic turbojet engine performance comparison is shown with convergent-divergent nozzles of varying efficiencies. It is seen that at Mach 1 and 2 the convergent-divergent nozzle engine performance is inferior to the convergent nozzle engine and it is only at Mach 3.0 (as shown in Fig. 26) that the expanding nozzle enjoys an advantage. The importance of nozzle efficiency is shown here also by comparing two C-D nozzles, one with an efficiency range of 85-95% and the other of 90-95%. For an actual engine design, however, it is realized that there would be more to compare between the two than just efficiency and specific thrust. For an actual installation the C-D nozzle would naturally take up much more space and weight and the practical aspects of designing such a nozzle with the variable geometry necessary for

efficient flight at varying conditions would not be a small undertaking. The results of this study indicate however, the importance of designing a nozzle with the maximum possible efficiency for an engine using a convergent-divergent nozzle.

5. CONCLUSIONS

As a result of the calculations made in this study of the afterburning turbofan there are several conclusions to be drawn as to the performance characteristics of the turbofan when used for propelling aircraft in the Mach 2-3 flight regime.

1. In the speed range from Mach 2 to 3 the by-pass afterburning turbofan engine shows a definite performance advantage over the straight turbojet. For instance, at 70,000 feet and a flight Mach number of 3.0, the specific thrust of the turbofan engine is 15% greater than that of the conventional turbojet.

2. The engine with a compression ratio of 6 is to be preferred over the high compression engine in all phases of supersonic flight. At a compression of 6.0 an engine has a specific thrust that is 6% greater than a similar engine with a compression ratio of 16.0 at 60,000 feet and a flight Mach number of 2.0.

3. From the transonic speed region to approximately Mach 2, the turbofan engine is inferior to the turbojet. At 50,000 feet, the specific thrust of the turbojet is approximately 9% better than that of the turbofan at a flight Mach number of 1.0. As speed is increased to 2.0, the performance of the two engines is essentially equal and at Mach 3.0 the turbofan has a specific thrust that is 6% greater than the turbojet.

4. Fan pressure ratios have little effect on engine performance in high speed flight. Engine designs should therefore consider that pressure ratio which is the most desirable for lower flight speeds. This study shows a performance advantage of the turbofan engine with a fan pressure ratio of 1.7 at the Mach 1.0 flight regime.

5. The performance advantage of an engine with a given by-pass ratio when compared to a similar engine with a different by-pass ratio is a function of flight Mach number. At Mach 1.0 the by-pass ratio of 1.0 is better and at Mach 3.0 the by-pass ratio 2.0 engine has a performance advantage. To choose the correct engine for a particular aircraft, the designer would have to arrive at a compromise between the

relative amounts of flight time to be spent at each flight speed and the performance difference in the various by-pass ratio engines. At 70,000 feet and a flight Mach number of 3.0, for instance, the specific thrust of the by-pass ratio 2.0 engine is 4% greater than that of the by-pass ratio 1.0 engine.

6. At a flight Mach number of 3.0 the performance of the combination ram-turbojet engine is essentially equal to that of the turbofan. The specific thrust of the turbofan engine at 40,000 feet and a flight Mach number of 1.0 is 25% greater than that of the ram-turbojet.

7. Engine performance could be greatly improved if present turbine inlet temperatures could be raised. This improvement is true even for very high temperatures when energy losses occur because of dissociation.

8. For high speed flight in the Mach 3 region, and beyond, the convergent-divergent nozzle should be considered in the engine design. The efficiency of such a nozzle would have to closely approximate that of a convergent nozzle in order to realize a performance advantage for the convergent-divergent nozzle engine even at high Mach number flight.

6. REFERENCES

1. Hesse, Walter J., Jet Propulsion, 1st ed., Pitman Publishing Corporation, New York, 1958.

2. Convenient Gas Properties and Charts for Gas Turbine Calculations, Walker, Chapman J., The American Society of Mechanical Engineers, Paper Number 50-F-28, 1950.

3. Air Intake Problems in Supersonic Propulsion, Advisory Group for Aeronautical Research and Development, North Atlantic Treaty Organization (AGARD), Pergamon Press, New York, 1958.

4. Properties of Combustion Gases, General Electric Company, McGraw-Hill Book Company, Inc., New York, 1955.

Fig. 1

PROPULSIVE EFFICIENCY COMPARISON

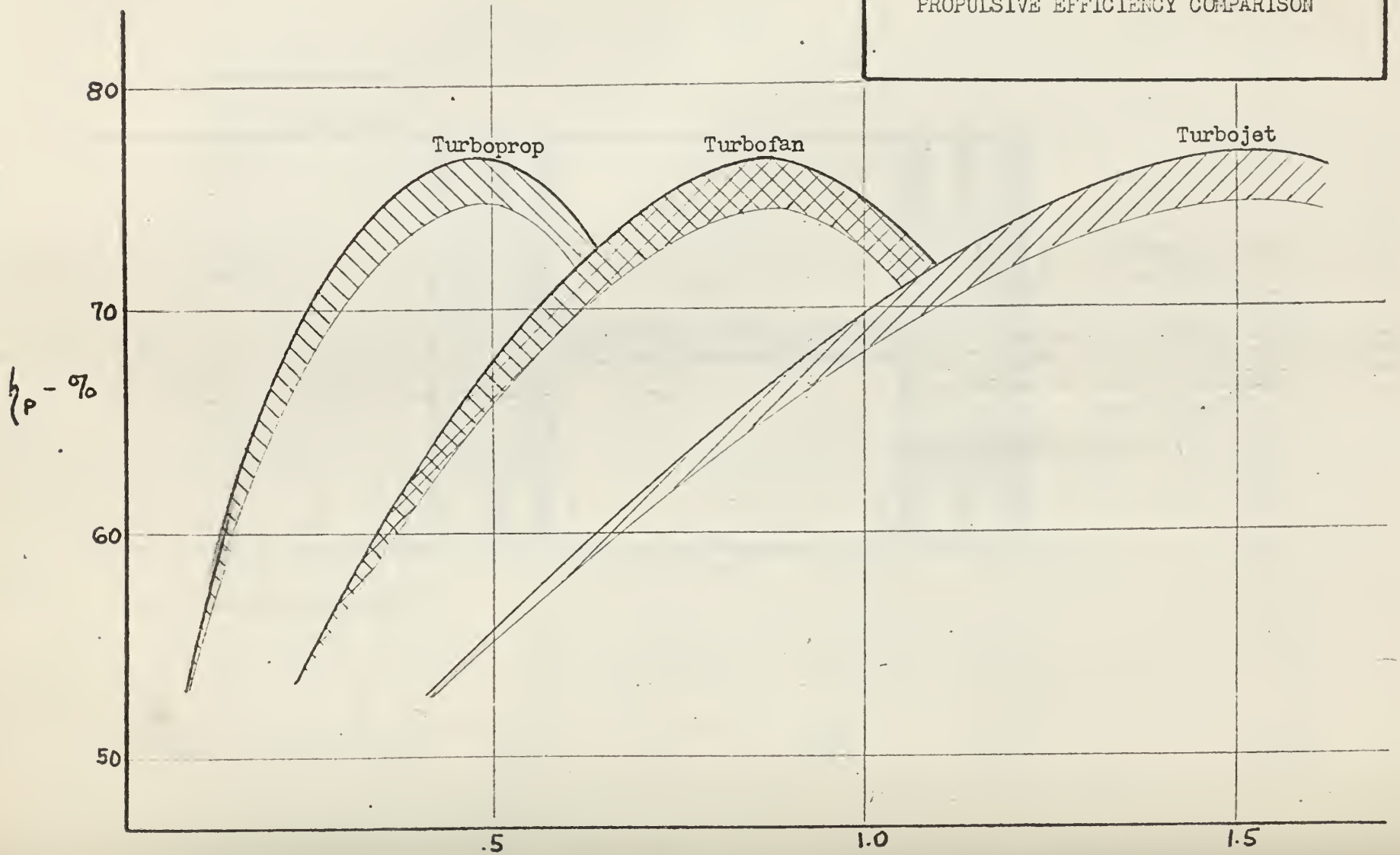

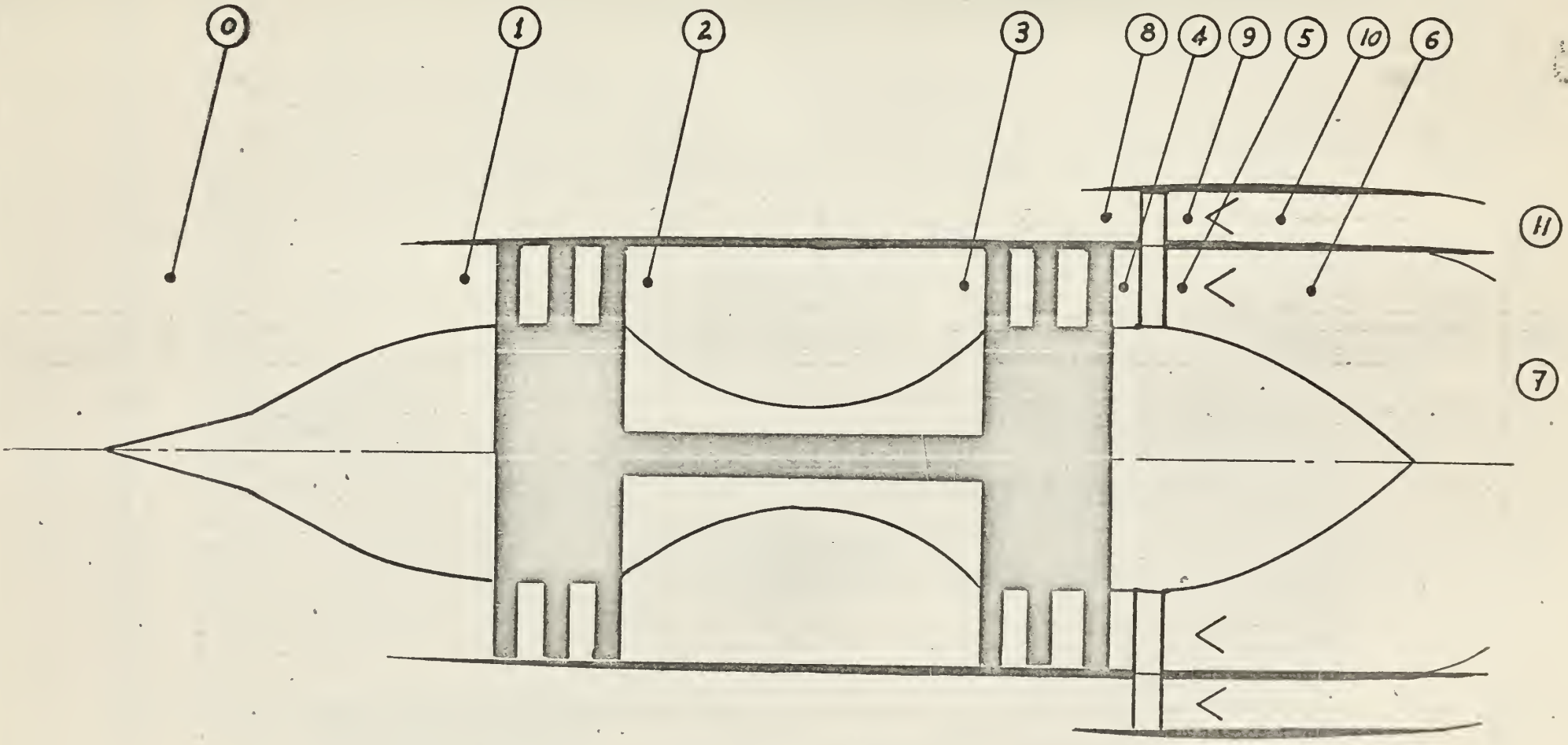

FIG. 2

TURBOFAN ENGINE WITH AFTERBURNING

STATIONS NUMBERED AS DESIGNATED IN THE CALCULATIONS

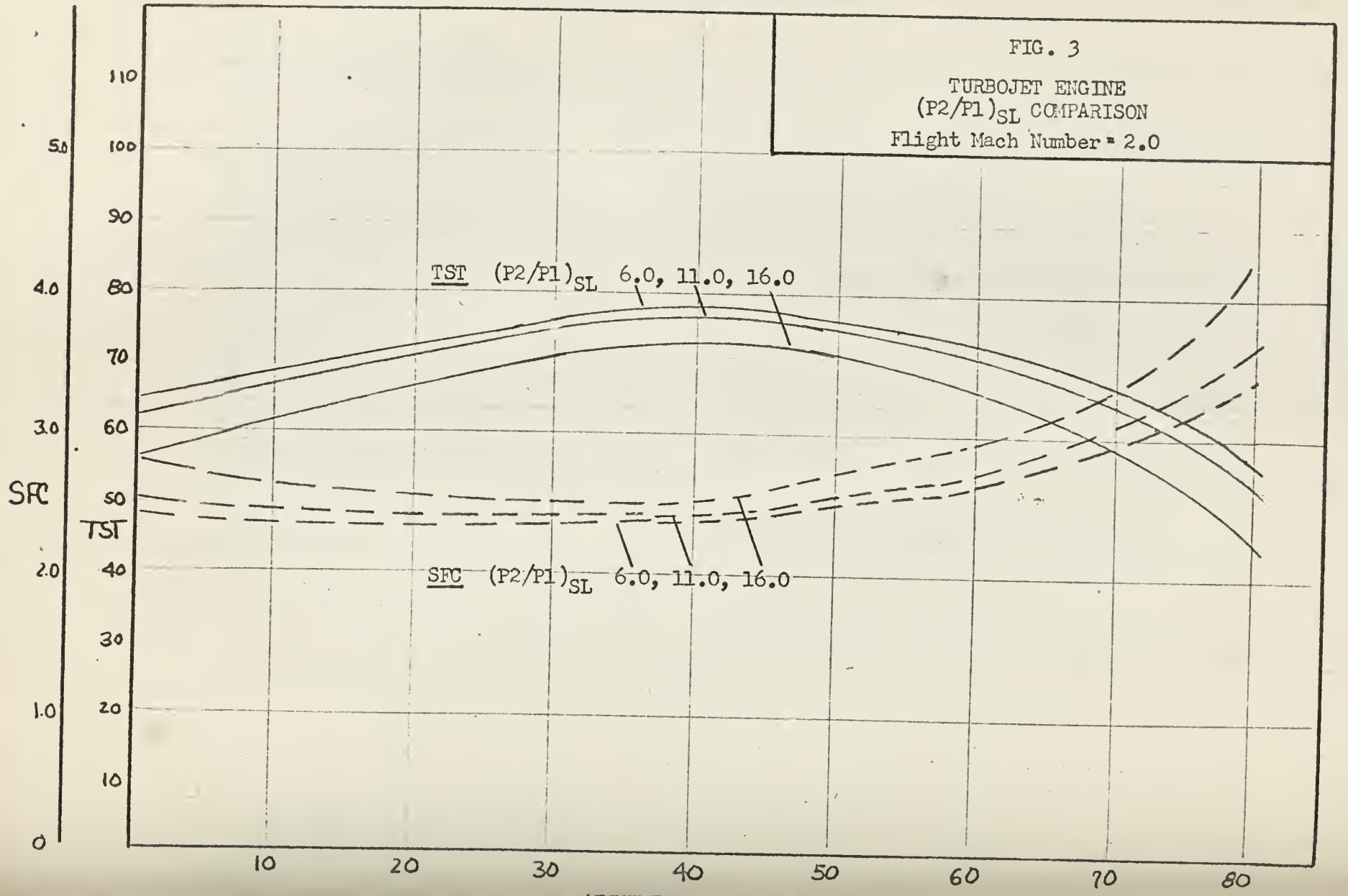
FIG. 3
TURBOJET ENGINE
$(P2/P1)_{SL}$ COMPARISON
Flight Mach Number = 2.0
TST $(P2/P1)_{SL}$ 6.0, 11.0, 16.0
SFC $(P2/P1)_{SL}$ 6.0, 11.0, 16.0
SFC
TST
ALTITUDE - 1000's Ft.
0
1.0
2.0
3.0
4.0
5.0
10
20
30
40
50
60
70
80
90
100
110
10
20
30
40
50
60
70
80

FIG. 5

COMPRESSOR PRESSURE RATIO
With Varying Altitude and Mach No.

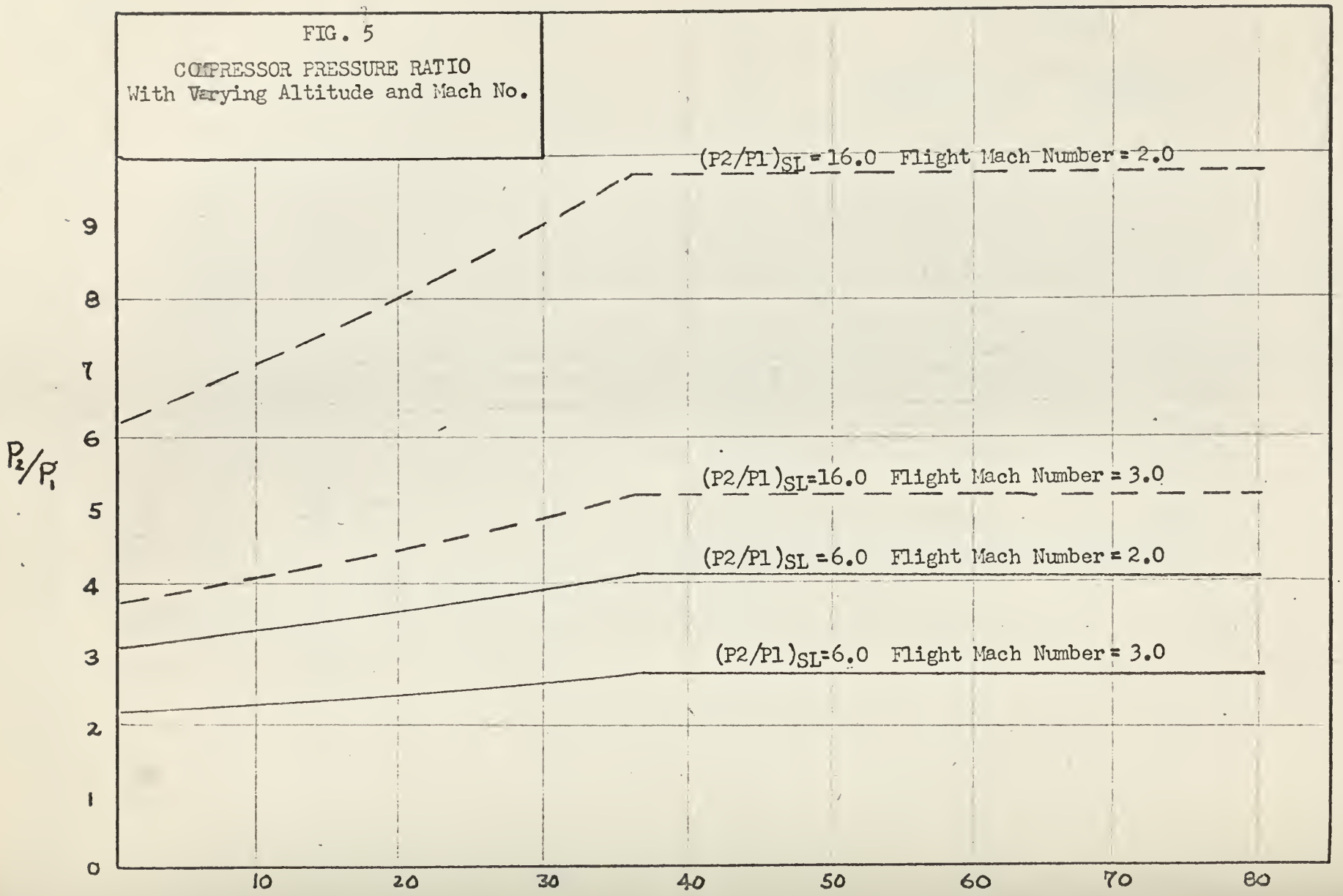

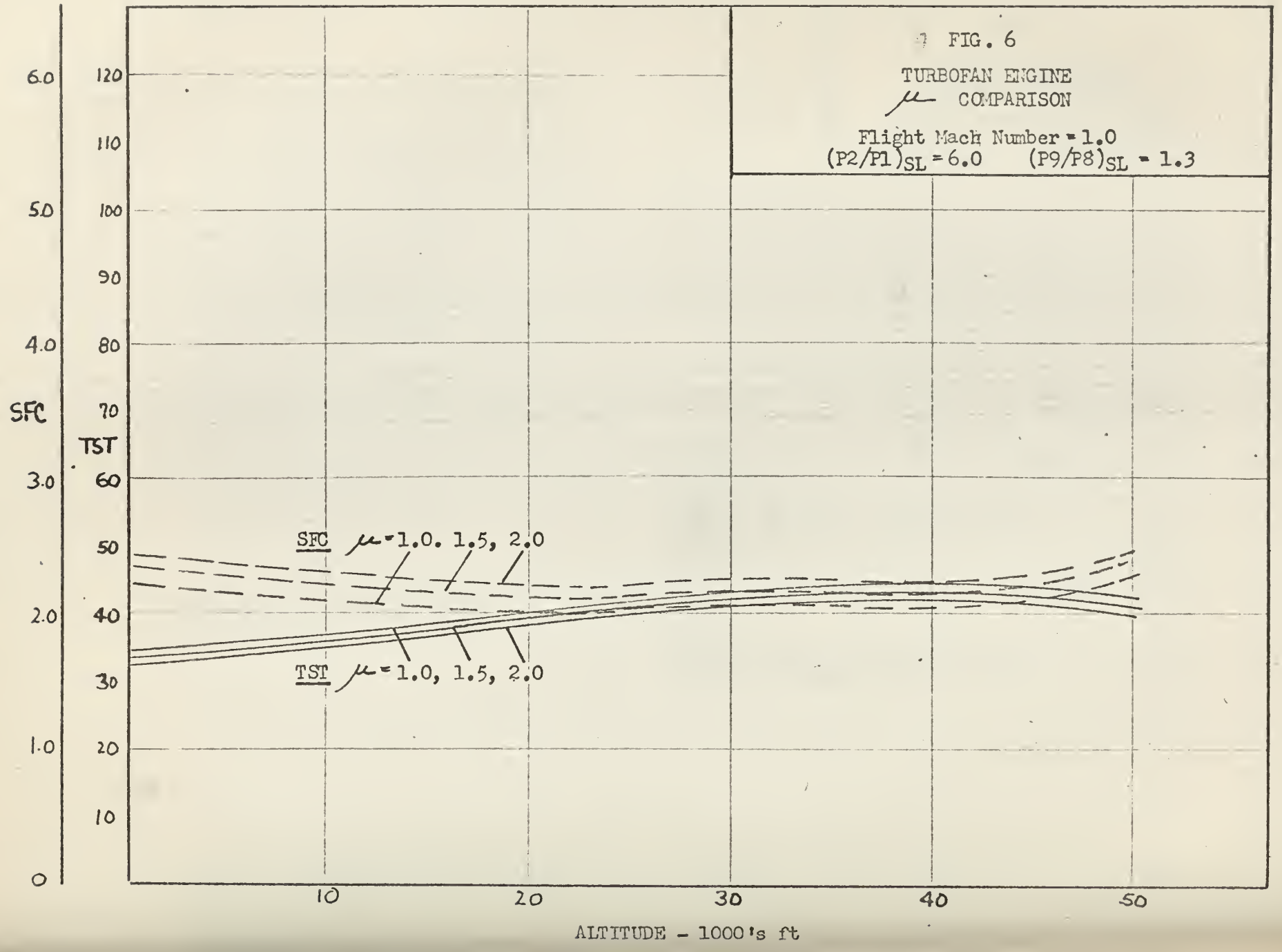
FIG. 6
TURBOFAN ENGINE
μ COMPARISON
Flight Mach Number = 1.0
(P2/P1)SL = 6.0 (P9/P8)SL = 1.3
SFC μ=1.0, 1.5, 2.0
TST μ=1.0, 1.5, 2.0
SFC
TST
6.0
5.0
4.0
3.0
2.0
1.0
0
120
110
100
90
80
70
60
50
40
30
20
10
10
20
30
40
50
ALTITUDE - 1000's ft

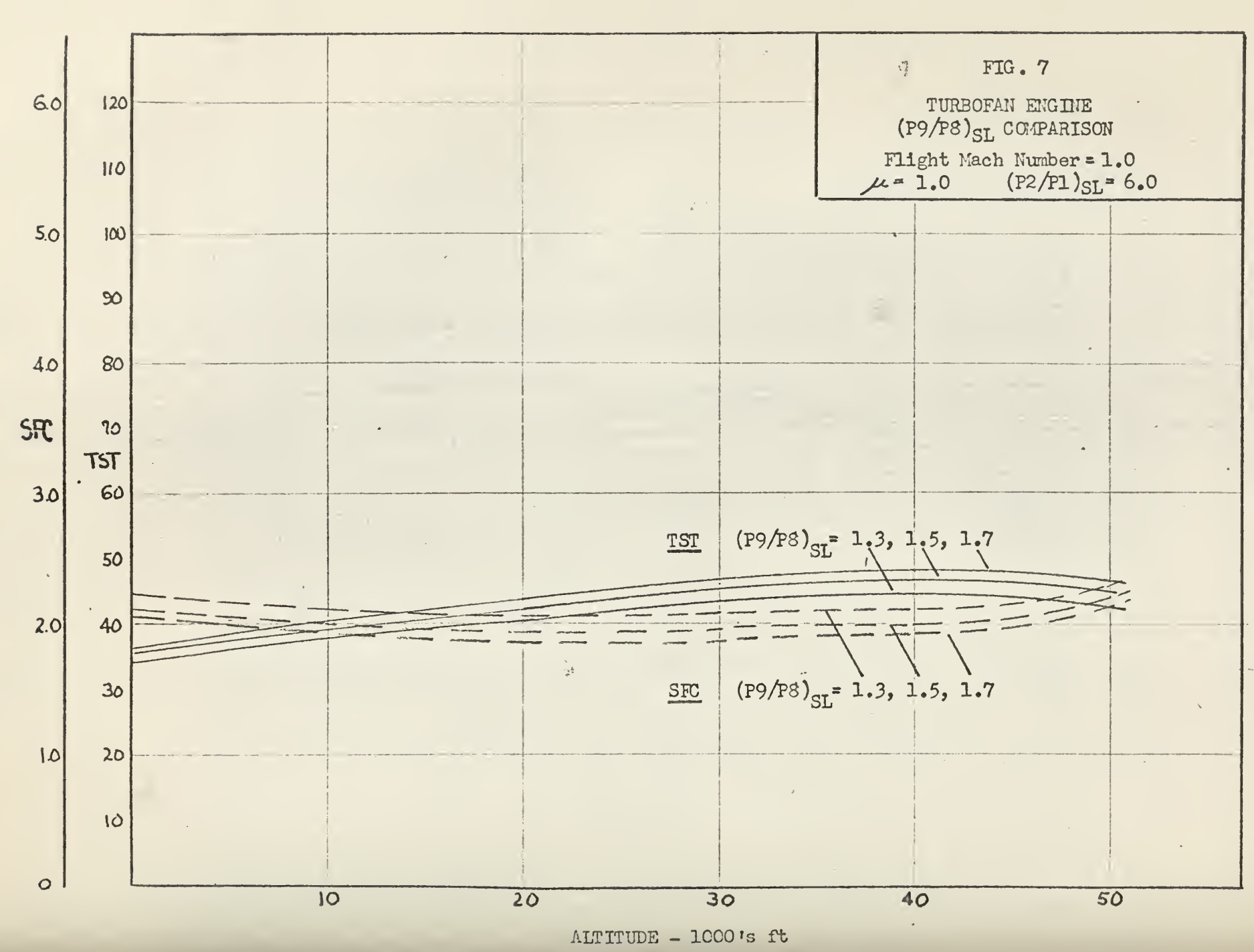
FIG. 7
TURBOFAN ENGINE
$(P9/P8)_{SL}$ COMPARISON
Flight Mach Number = 1.0
μ = 1.0 $(P2/P1)_{SL}$ = 6.0
TST $(P9/P8)_{SL}$ = 1.3, 1.5, 1.7
SFC $(P9/P8)_{SL}$ = 1.3, 1.5, 1.7
SFC
TST
6.0
5.0
4.0
3.0
2.0
1.0
0
120
110
100
90
80
70
60
50
40
30
20
10
10
20
30
40
50
ALTITUDE - 1000's ft

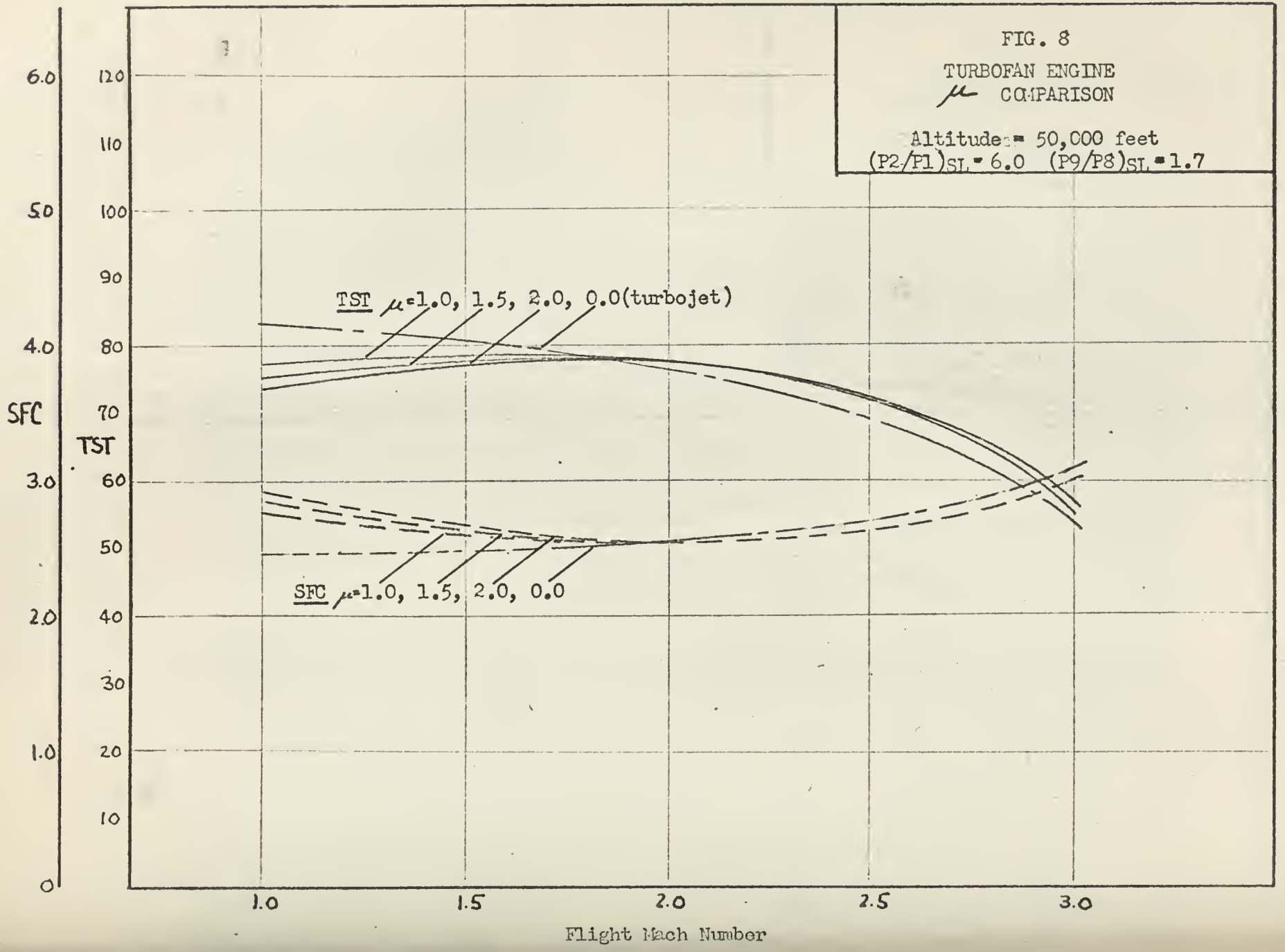
FIG. 8
TURBOFAN ENGINE
μ COMPARISON
Altitude = 50,000 feet
(P2/P1)SL = 6.0 (P9/P8)SL = 1.7
TST μ=1.0, 1.5, 2.0, 0.0(turbojet)
SFC μ=1.0, 1.5, 2.0, 0.0
SFC
TST
6.0
5.0
4.0
3.0
2.0
1.0
0
120
110
100
90
80
70
60
50
40
30
20
10
1.0
1.5
2.0
2.5
3.0
Flight Mach Number

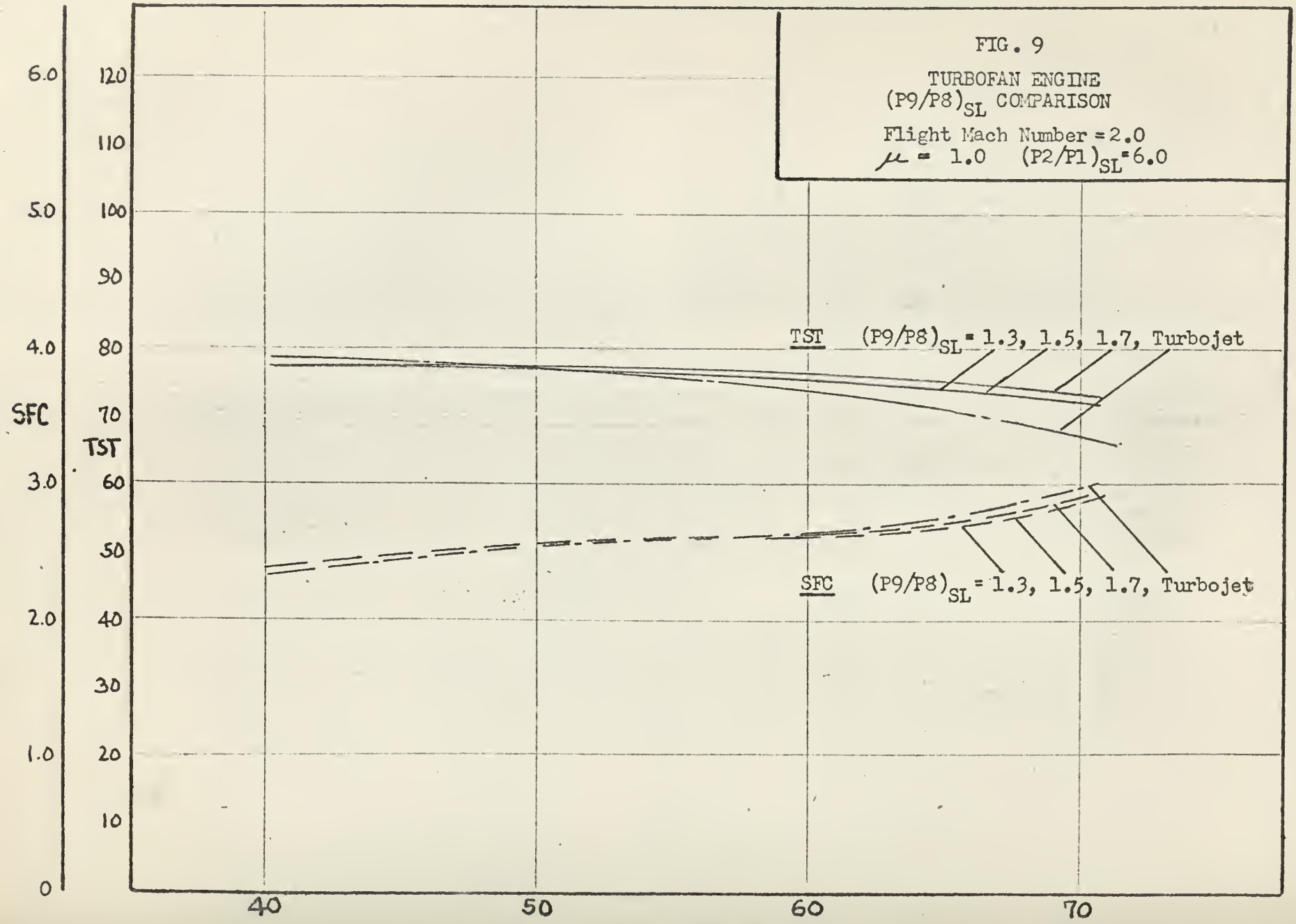
FIG. 9
TURBOFAN ENGINE
$(P9/P8)_{SL}$ COMPARISON
Flight Mach Number = 2.0
μ = 1.0 $(P2/P1)_{SL}$ = 6.0
TST $(P9/P8)_{SL}$ = 1.3, 1.5, 1.7, Turbojet
SFC $(P9/P8)_{SL}$ = 1.3, 1.5, 1.7, Turbojet
SFC
TST
6.0
5.0
4.0
3.0
2.0
1.0
0
120
110
100
90
80
70
60
50
40
30
20
10
40
50
60
70
ALTITUDE - 1000's ft

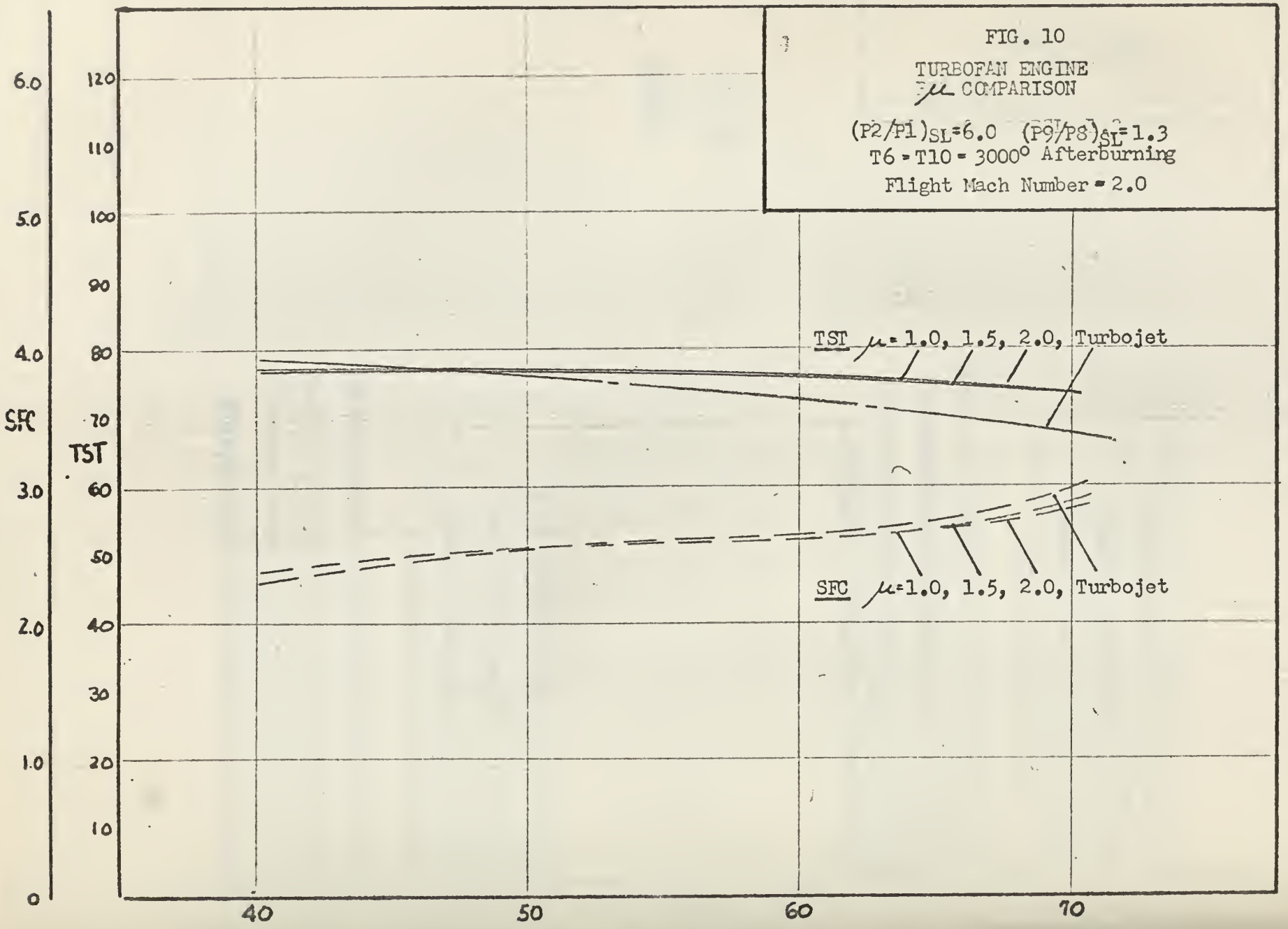
FIG. 10
TURBOFAN ENGINE
COMPARISON
$(P2/P1)_{SL}=6.0$ $(P9/P8)_{SL}=1.3$
T6 = T10 = 3000° Afterburning
Flight Mach Number = 2.0
TST μ = 1.0, 1.5, 2.0, Turbojet
SFC μ = 1.0, 1.5, 2.0, Turbojet
SFC
TST
ALTITUDE - 1000's ft
6.0
5.0
4.0
3.0
2.0
1.0
0
120
110
100
90
80
70
60
50
40
30
20
10
40
50
60
70

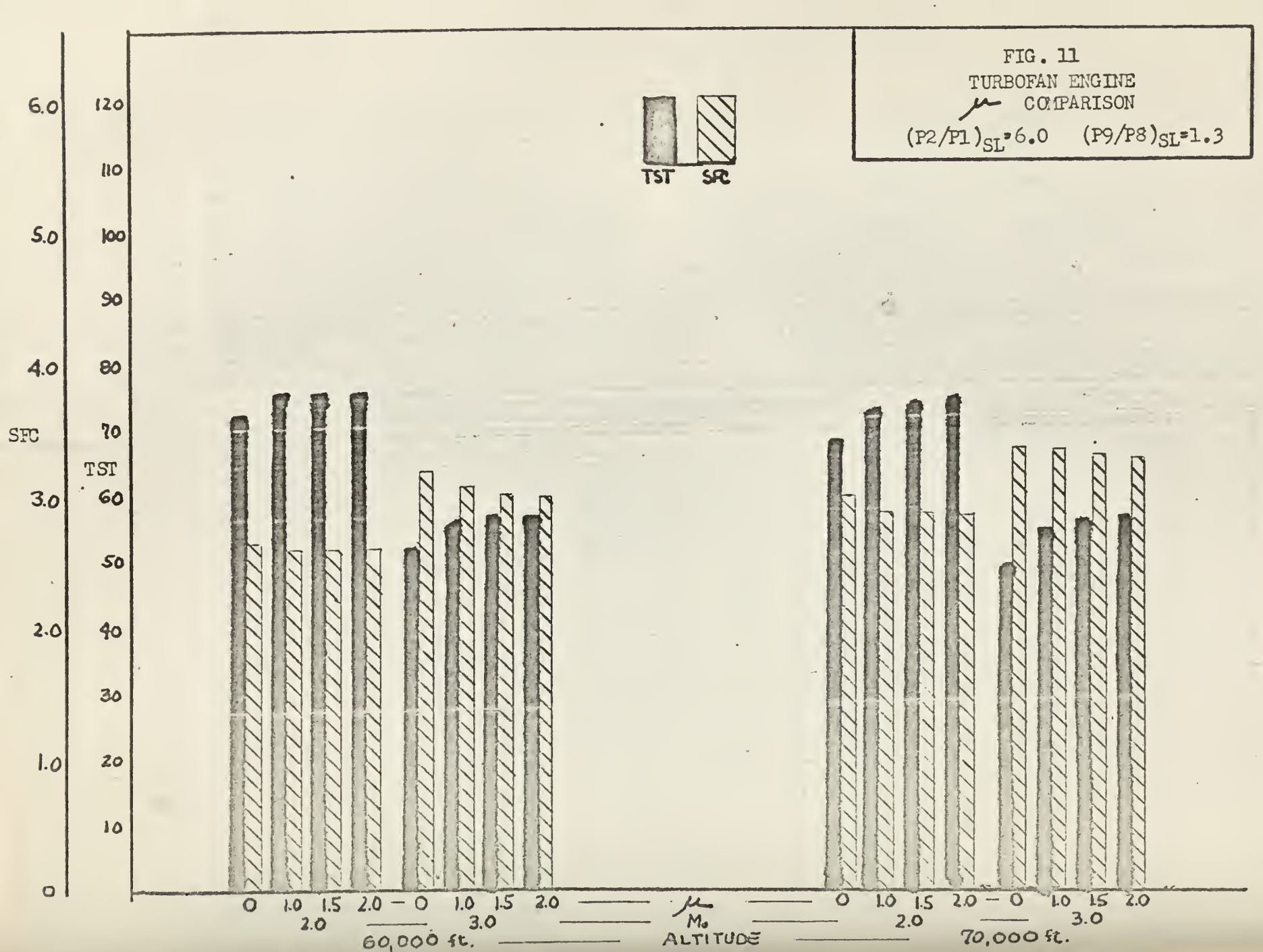
FIG. 11
TURBOFAN ENGINE
μ COMPARISON
$(P2/P1)_{SL}$=6.0 $(P9/P8)_{SL}$=1.3
TST
SFC
SFC
TST
6.0
5.0
4.0
3.0
2.0
1.0
0
120
110
100
90
80
70
60
50
40
30
20
10
0 1.0 1.5 2.0 — 0 1.0 1.5 2.0 — μ — 0 1.0 1.5 2.0 — 0 1.0 1.5 2.0
2.0 — 3.0 — M_0 — 2.0 — 3.0
60,000 ft. — ALTITUDE — 70,000 ft.

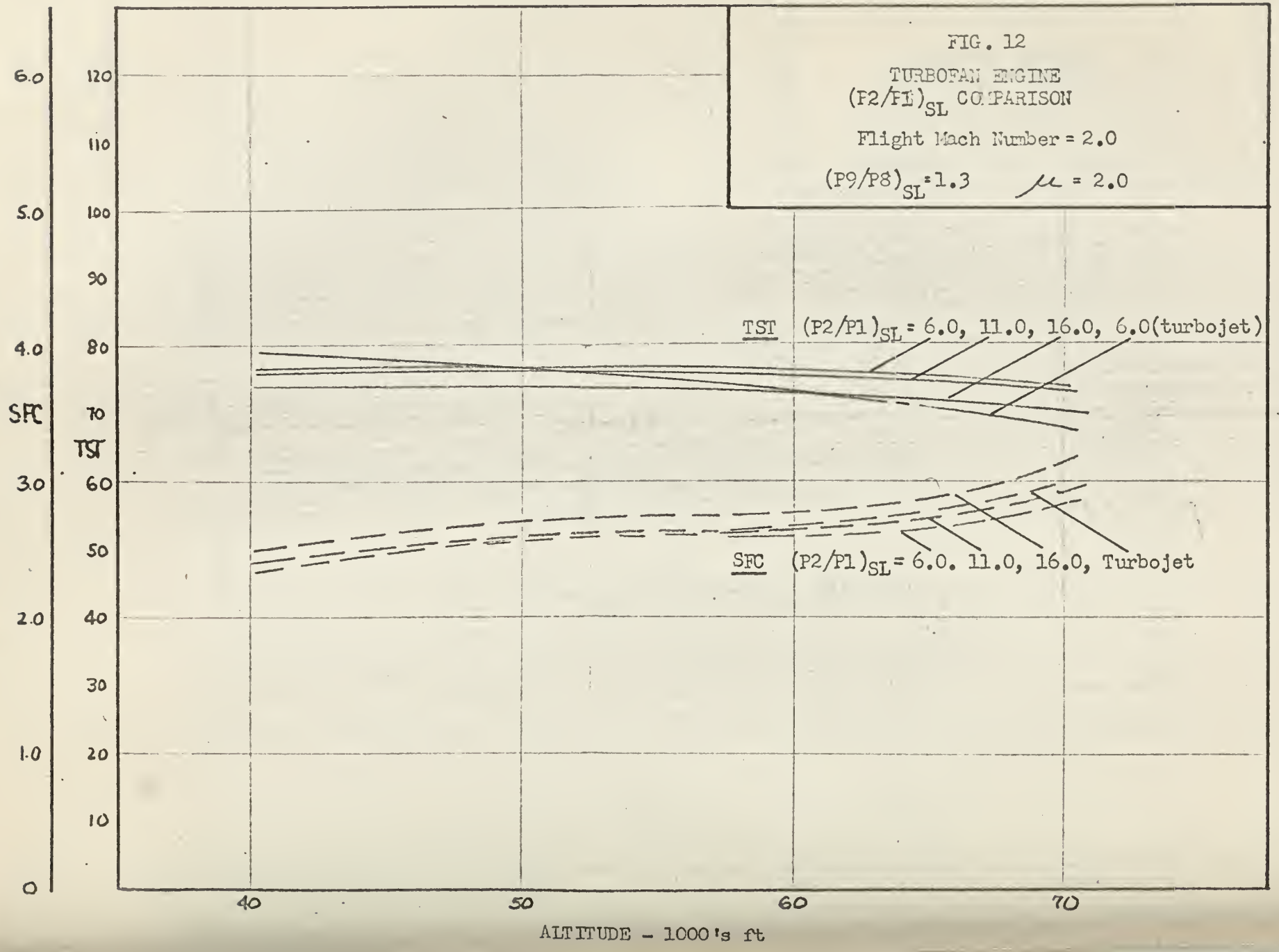
FIG. 12
TURBOFAN ENGINE
$(P2/P1)_{SL}$ COMPARISON
Flight Mach Number = 2.0
$(P9/P8)_{SL}$ = 1.3 μ = 2.0
TST $(P2/P1)_{SL}$ = 6.0, 11.0, 16.0, 6.0(turbojet)
SFC $(P2/P1)_{SL}$ = 6.0. 11.0, 16.0, Turbojet
SFC
TST
6.0
5.0
4.0
3.0
2.0
1.0
0
120
110
100
90
80
70
60
50
40
30
20
10
40
50
60
70
ALTITUDE - 1000's ft

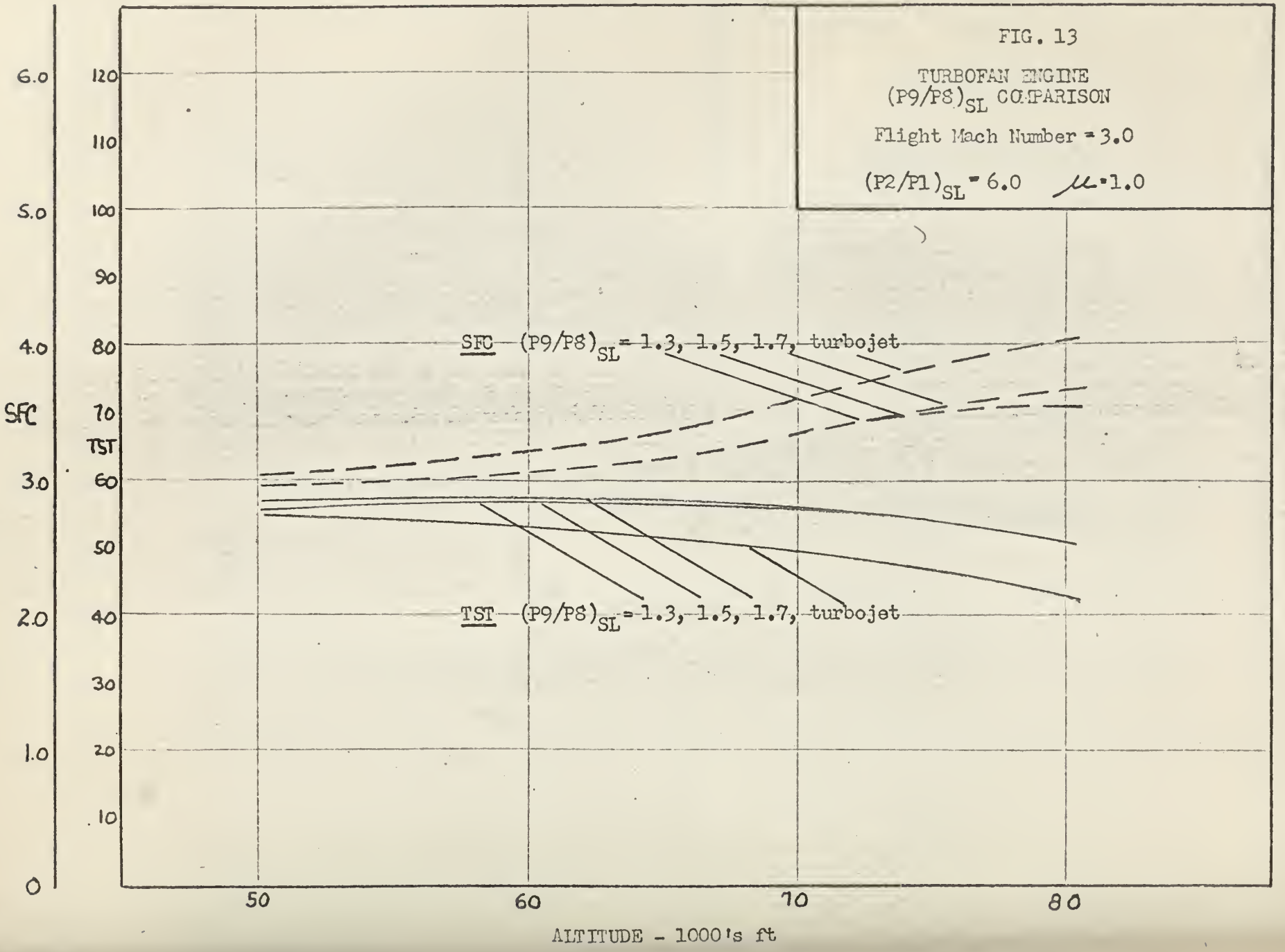
FIG. 13
TURBOFAN ENGINE
$(P9/P8)_{SL}$ COMPARISON
Flight Mach Number = 3.0
$(P2/P1)_{SL}$ = 6.0 μ = 1.0
SFC $(P9/P8)_{SL}$ = 1.3, 1.5, 1.7, turbojet
TST $(P9/P8)_{SL}$ = 1.3, 1.5, 1.7, turbojet
SFC
TST
6.0
5.0
4.0
3.0
2.0
1.0
0
120
110
100
90
80
70
60
50
40
30
20
10
50
60
70
80
ALTITUDE - 1000's ft

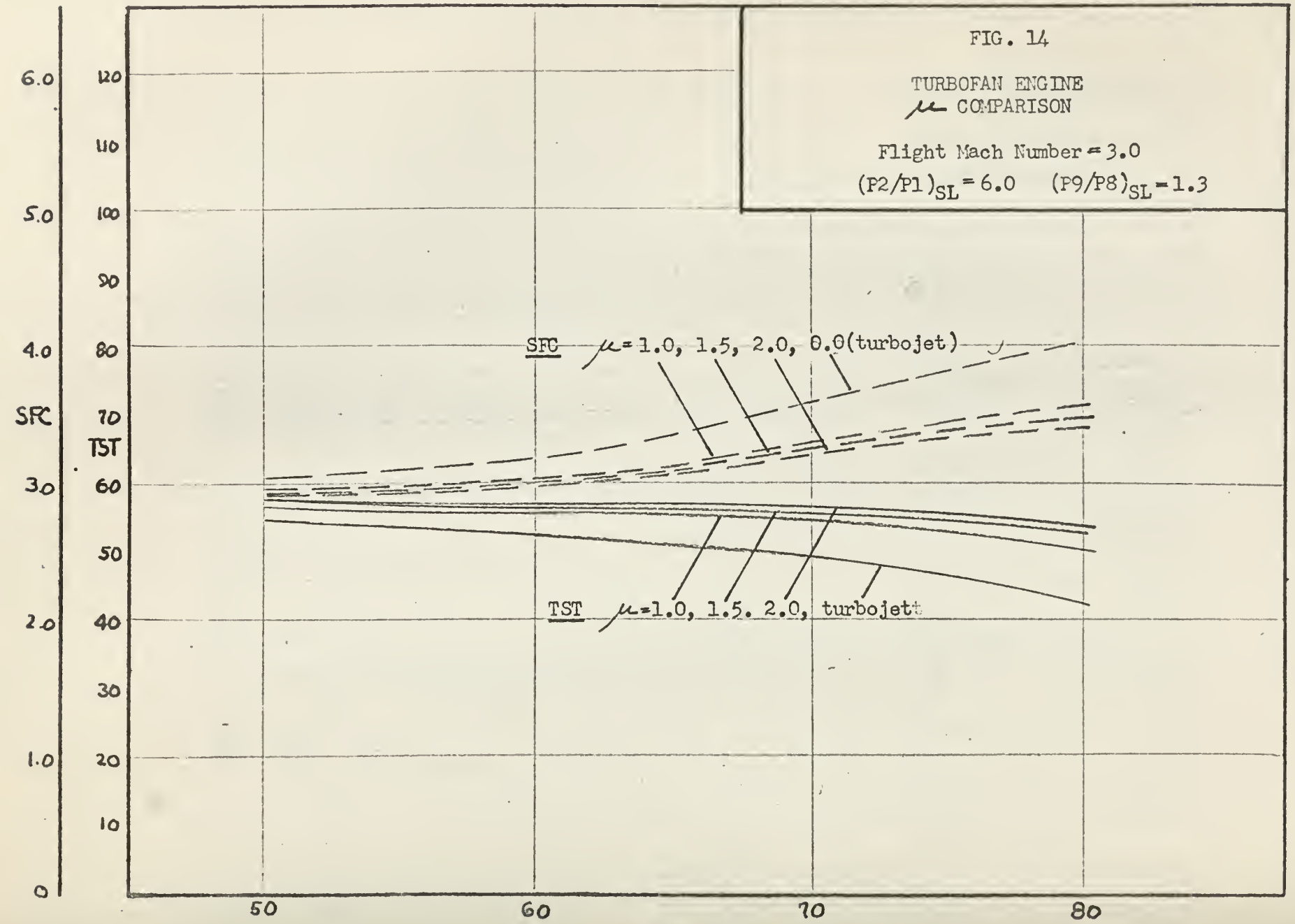
FIG. 14
TURBOFAN ENGINE
μ COMPARISON
Flight Mach Number = 3.0
(P2/P1)SL = 6.0 (P9/P8)SL = 1.3
SFC μ = 1.0, 1.5, 2.0, 0.0(turbojet)
TST μ = 1.0, 1.5. 2.0, turbojet
SFC
TST
6.0
5.0
4.0
3.0
2.0
1.0
0
120
110
100
90
80
70
60
50
40
30
20
10
50
60
70
80
ALTITUDE - 1000's ft

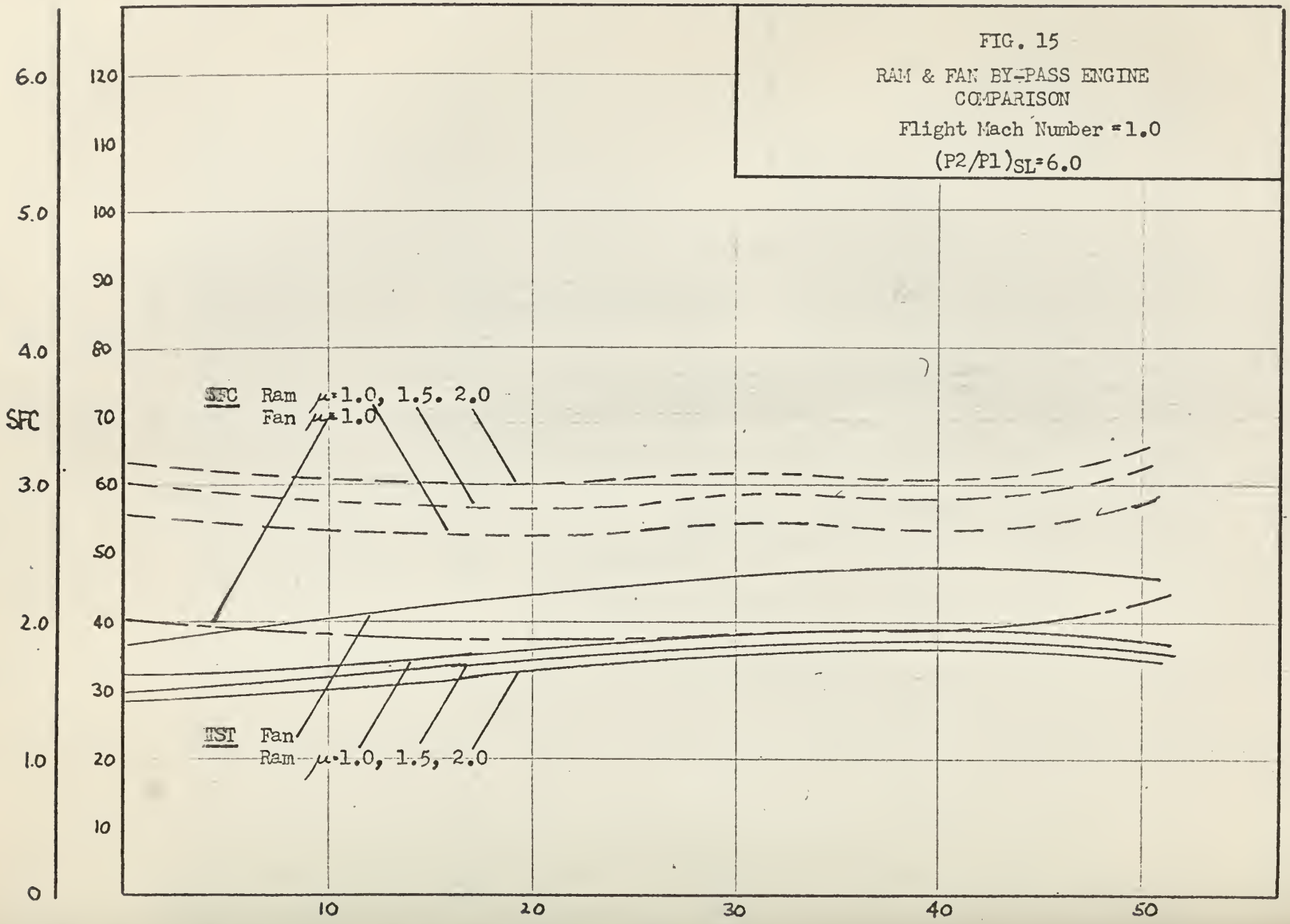
FIG. 15
RAM & FAN BY-PASS ENGINE COMPARISON
Flight Mach Number = 1.0
$(P2/P1)_{SL}$ = 6.0
SFC Ram μ=1.0, 1.5. 2.0
Fan μ=1.0
TST Fan
Ram μ=1.0, 1.5, 2.0
SFC
TST
6.0
5.0
4.0
3.0
2.0
1.0
0
120
110
100
90
80
70
60
50
40
30
20
10
10
20
30
40
50
ALTITUDE - 1000's ft

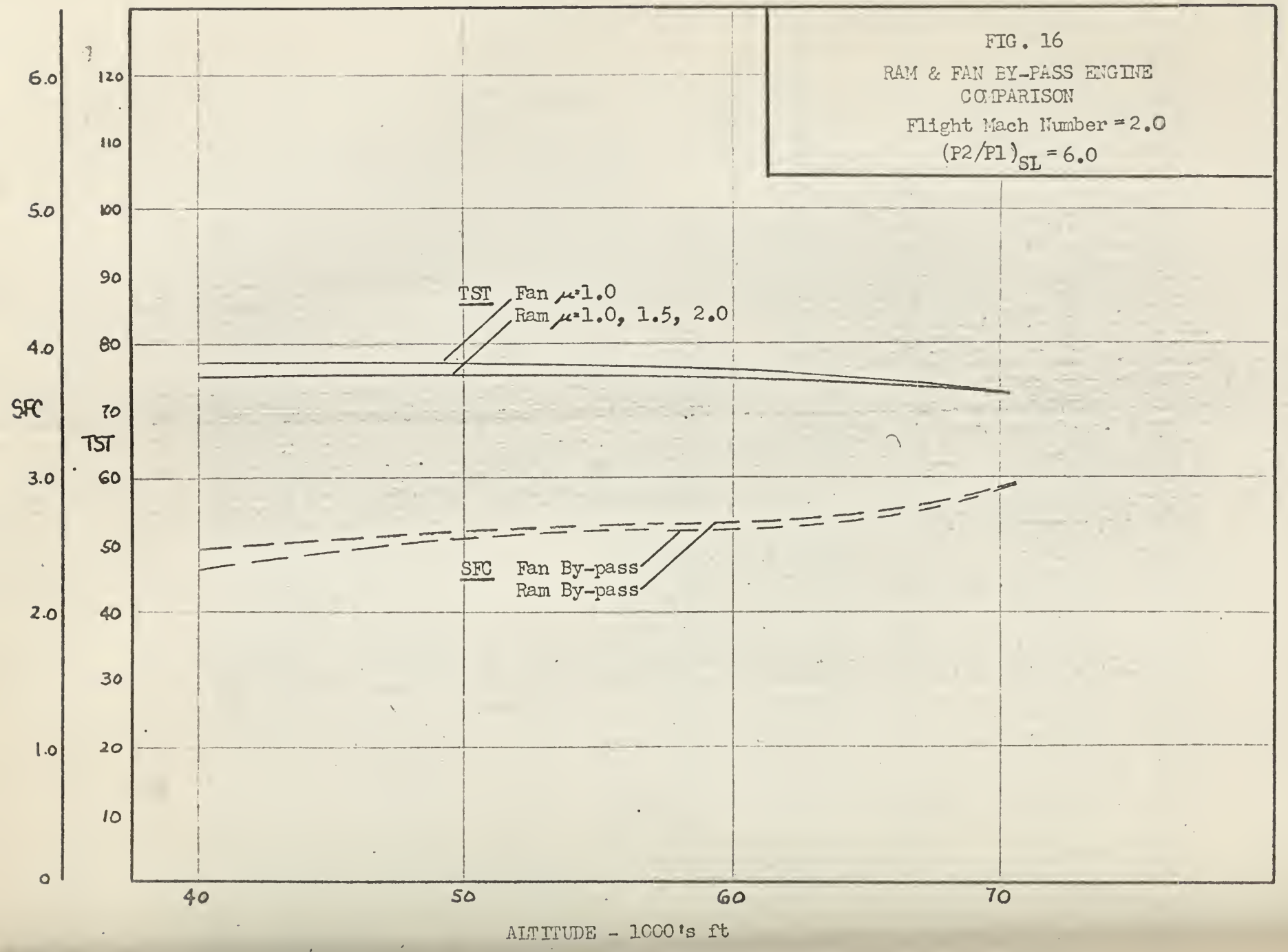
FIG. 16
RAM & FAN BY-PASS ENGINE
COMPARISON
Flight Mach Number = 2.0
$(P2/P1)_{SL}$ = 6.0
TST Fan μ=1.0
Ram μ=1.0, 1.5, 2.0
SFC Fan By-pass
Ram By-pass
SFC
TST
6.0
5.0
4.0
3.0
2.0
1.0
0
120
110
100
90
80
70
60
50
40
30
20
10
40
50
60
70
ALTITUDE - 1000's ft

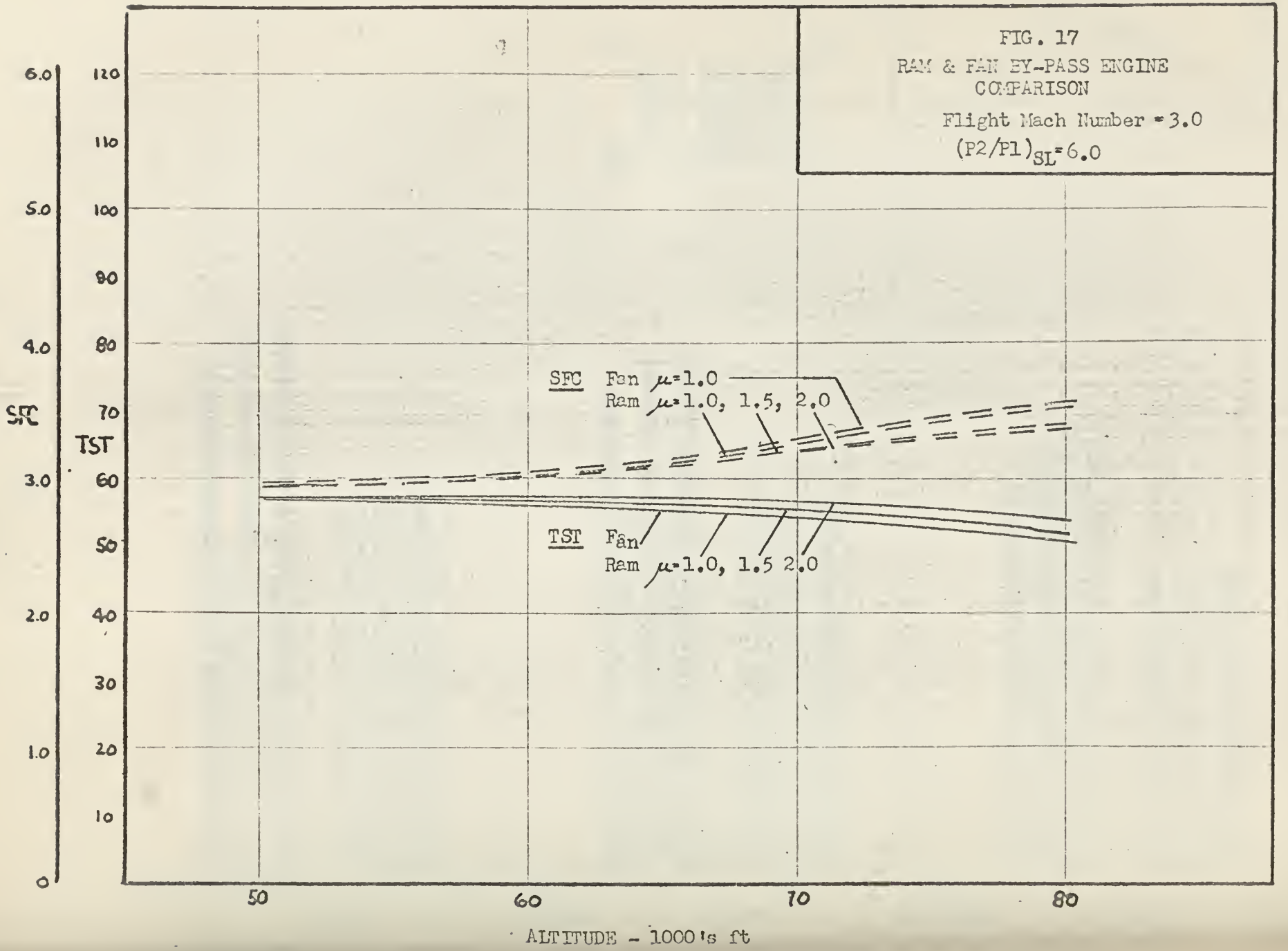
FIG. 17
RAM & FAN BY-PASS ENGINE
COMPARISON
Flight Mach Number = 3.0
$(P2/P1)_{SL}$ = 6.0
SFC Fan μ=1.0
Ram μ=1.0, 1.5, 2.0
TST Fan
Ram μ=1.0, 1.5 2.0
SFC
TST
6.0
5.0
4.0
3.0
2.0
1.0
0
120
110
100
90
80
70
60
50
40
30
20
10
50
60
70
80
ALTITUDE - 1000's ft

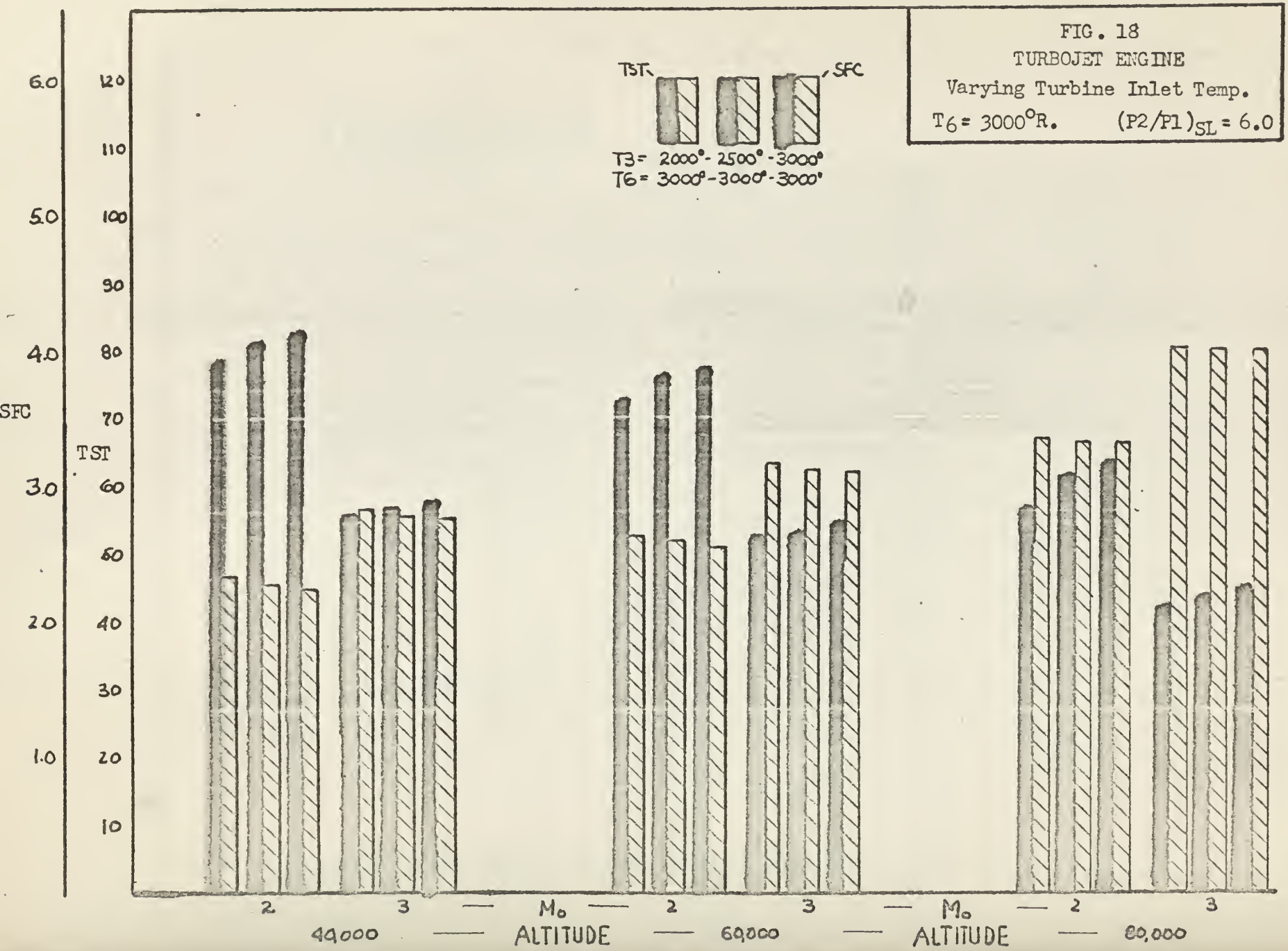
FIG. 18
TURBOJET ENGINE
Varying Turbine Inlet Temp.
T6 = 3000°R. (P2/P1)SL = 6.0
TST
SFC
T3 = 2000° - 2500° - 3000°
T6 = 3000° - 3000° - 3000°
SFC
TST
6.0
5.0
4.0
3.0
2.0
1.0
120
110
100
90
80
70
60
50
40
30
20
10
2
3
Mo
2
3
Mo
2
3
40,000
ALTITUDE
60,000
ALTITUDE
80,000

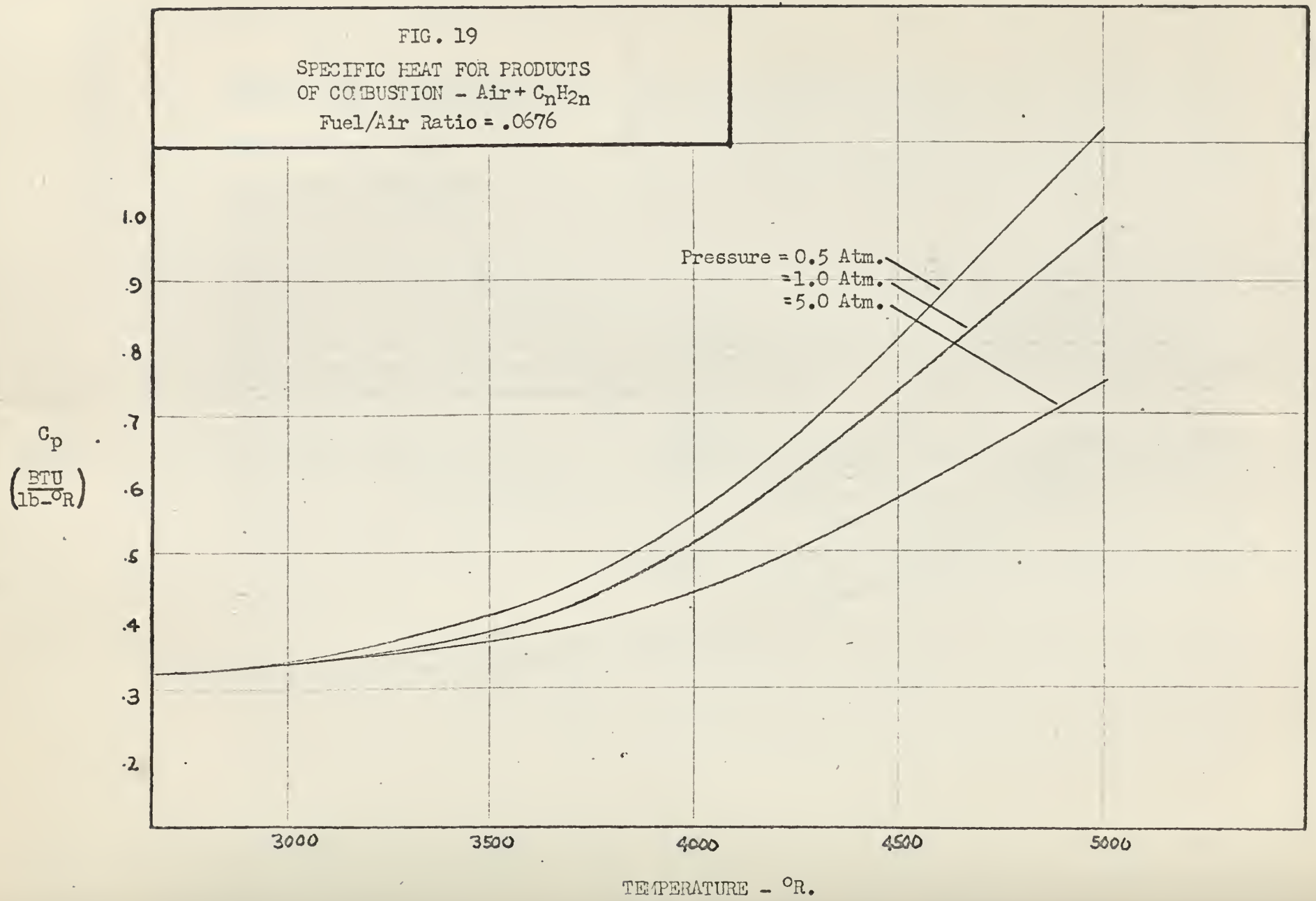
FIG. 19
SPECIFIC HEAT FOR PRODUCTS OF COMBUSTION - Air + C_nH_{2n}
Fuel/Air Ratio = .0676
Pressure = 0.5 Atm.
=1.0 Atm.
=5.0 Atm.
1.0
.9
.8
.7
.6
.5
.4
.3
.2
C_p
$\left(\frac{BTU}{lb-{}^oR}\right)$
3000
3500
4000
4500
5000
TEMPERATURE - ^oR.

FIG. 20

SPECIFIC HEAT FOR PRODUCTS OF COMBUSTION - Air + C_nH_{2n}

Varying Temperature and Fuel/Air Ratios

Pressure = 1 Atmosphere

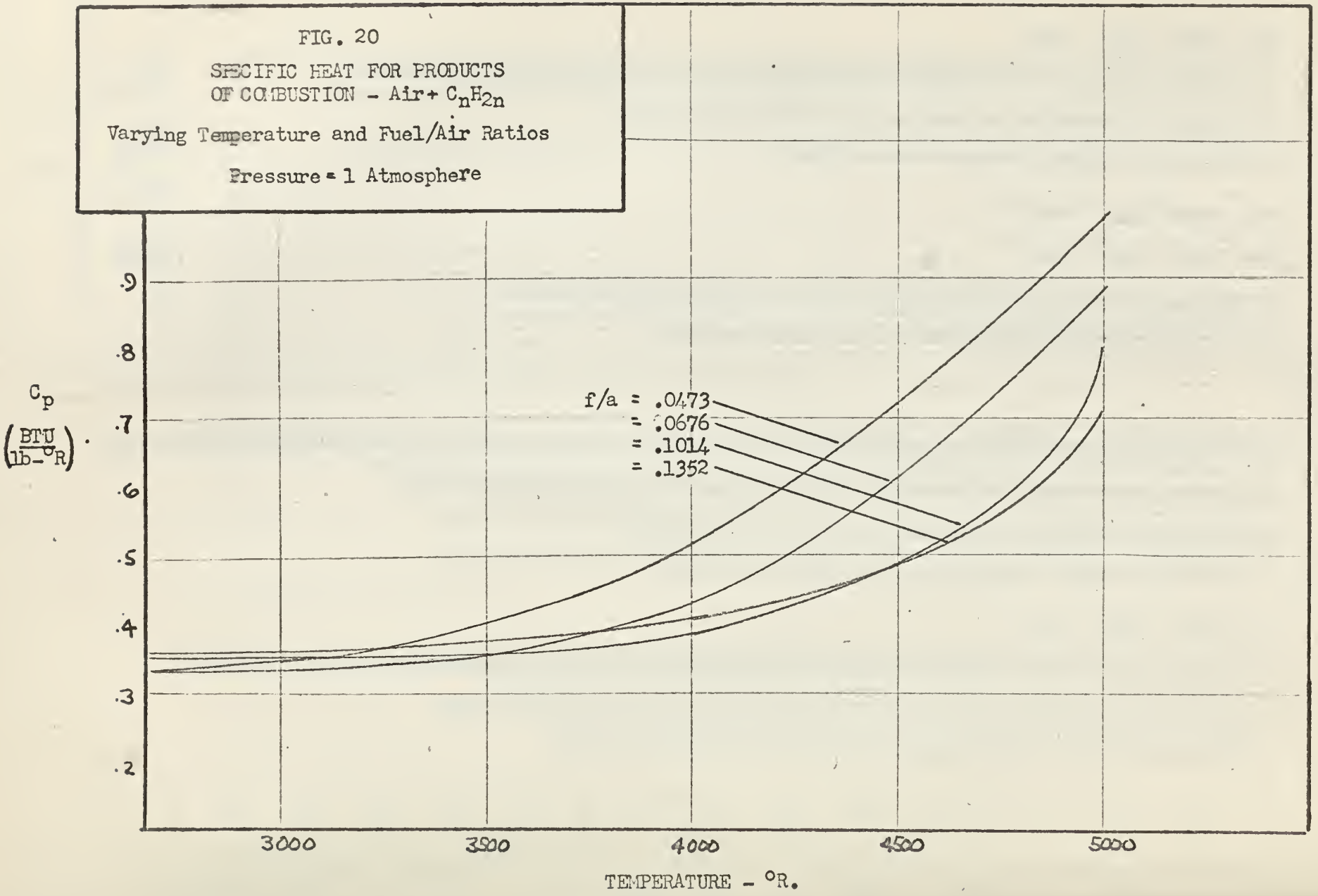

FIG. 21
TURBOJET ENGINE
Performance at High A/B Temp.

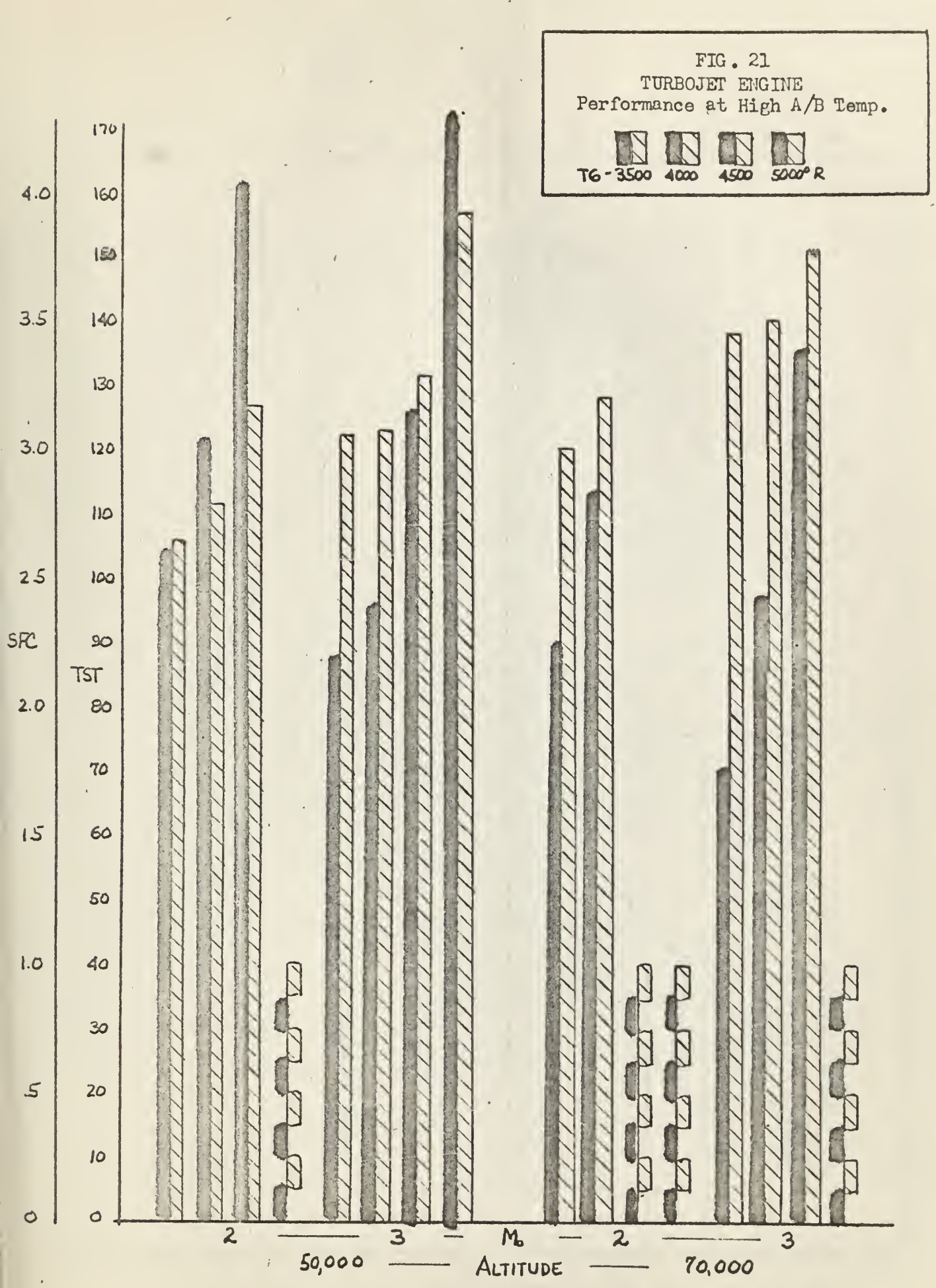

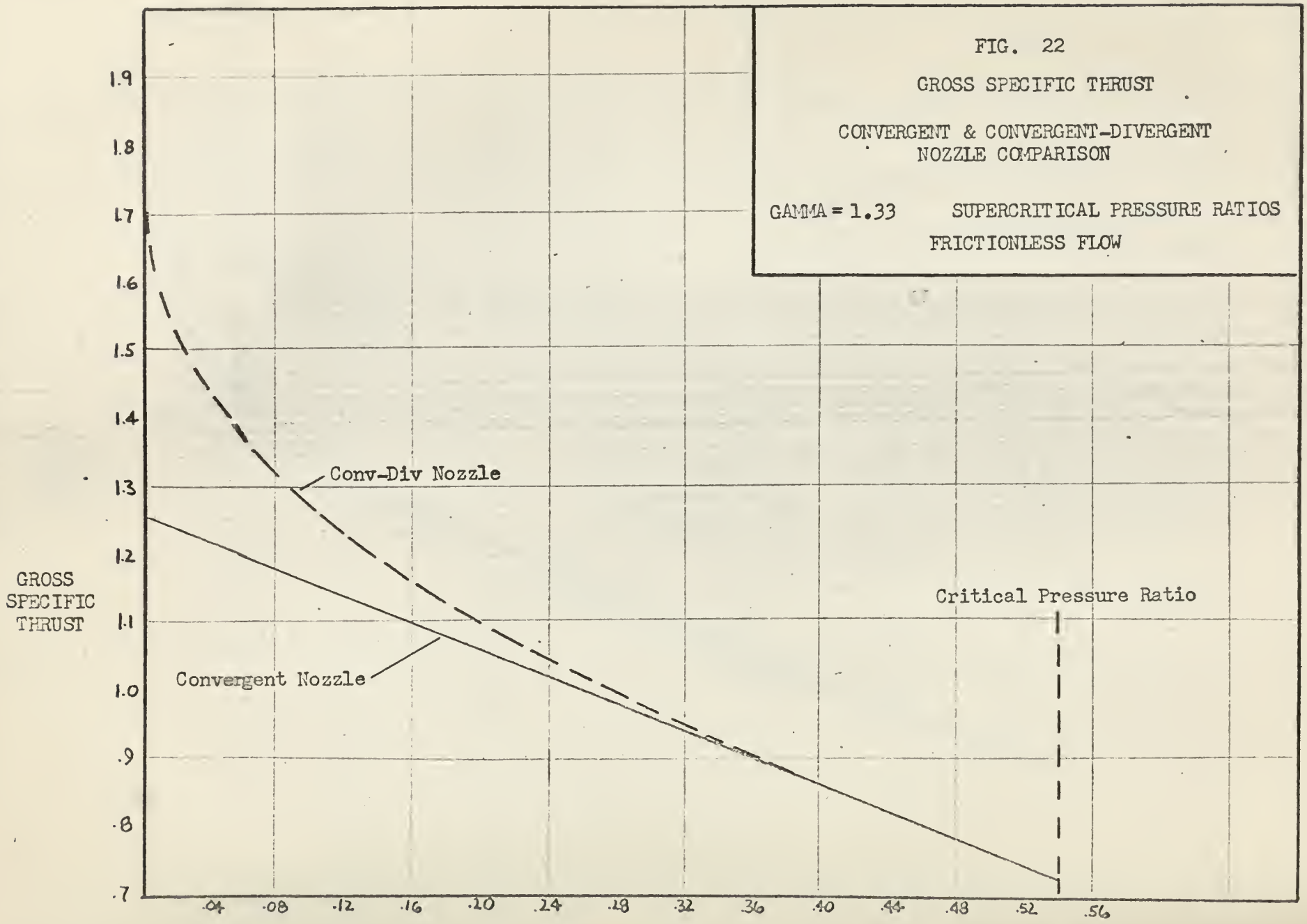
FIG. 22
GROSS SPECIFIC THRUST
CONVERGENT & CONVERGENT-DIVERGENT NOZZLE COMPARISON
GAMMA = 1.33 SUPERCRITICAL PRESSURE RATIOS
FRICTIONLESS FLOW
GROSS SPECIFIC THRUST
1.9
1.8
1.7
1.6
1.5
1.4
1.3
1.2
1.1
1.0
.9
.8
.7
Conv-Div Nozzle
Convergent Nozzle
Critical Pressure Ratio
.04
.08
.12
.16
.20
.24
.28
.32
.36
.40
.44
.48
.52
.56
NOZZLE PRESSURE RATIO - P_o/P_6

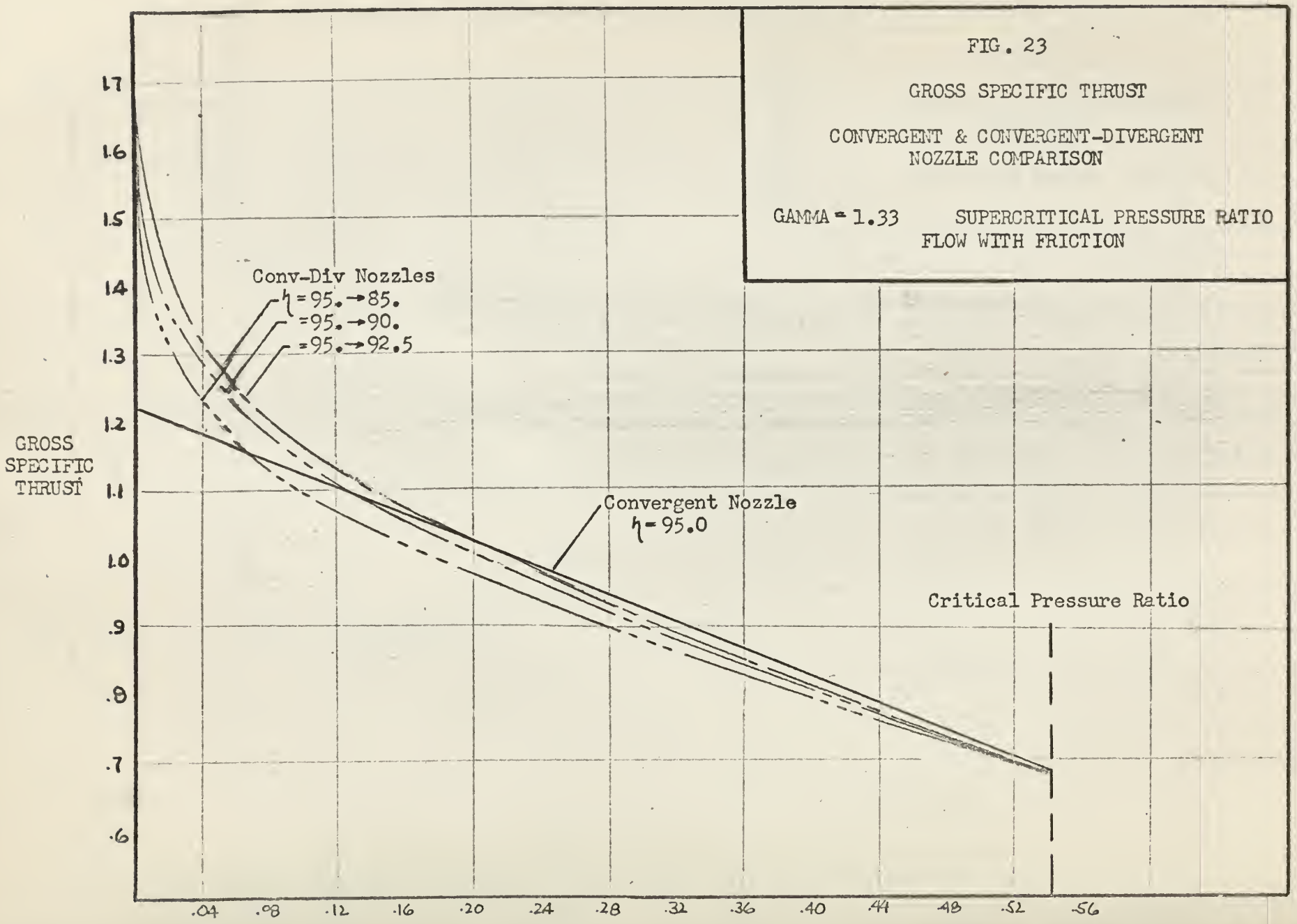
FIG. 23
GROSS SPECIFIC THRUST
CONVERGENT & CONVERGENT-DIVERGENT NOZZLE COMPARISON
GAMMA = 1.33 SUPERCRITICAL PRESSURE RATIO FLOW WITH FRICTION
Conv-Div Nozzles
η = 95. → 85.
= 95. → 90.
= 95. → 92.5
Convergent Nozzle
η = 95.0
Critical Pressure Ratio
GROSS SPECIFIC THRUST
1.7
1.6
1.5
1.4
1.3
1.2
1.1
1.0
.9
.8
.7
.6
.04
.08
.12
.16
.20
.24
.28
.32
.36
.40
.44
.48
.52
.56
NOZZLE PRESSURE RATIO - P_o/P_6

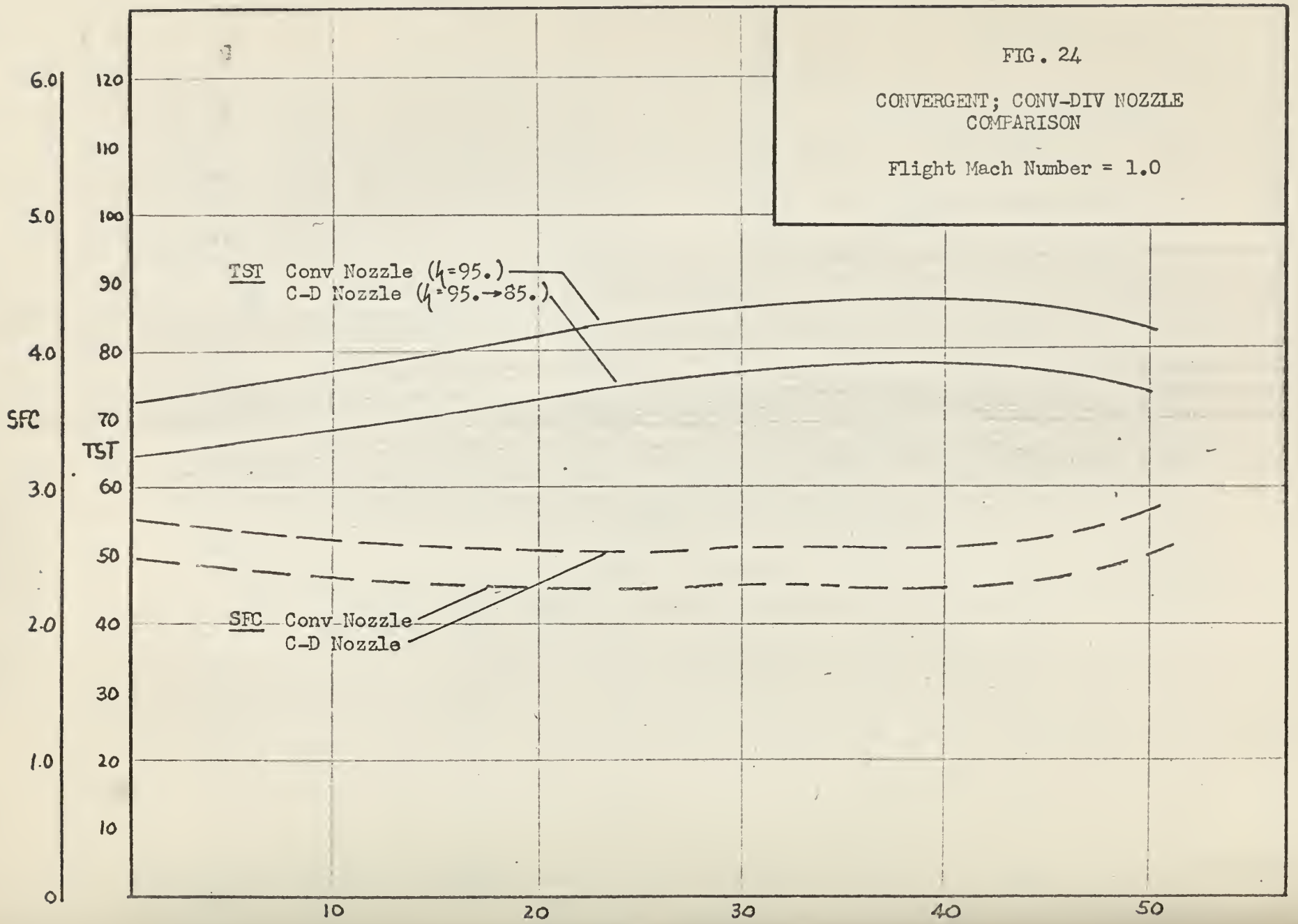
FIG. 24
CONVERGENT; CONV-DIV NOZZLE COMPARISON
Flight Mach Number = 1.0
TST Conv Nozzle (4=95.)
C-D Nozzle (4=95.→85.)
SFC Conv Nozzle
C-D Nozzle
SFC
TST
6.0
5.0
4.0
3.0
2.0
1.0
0
120
110
100
90
80
70
60
50
40
30
20
10
10
20
30
40
50
ALTITUDE - 1000's ft

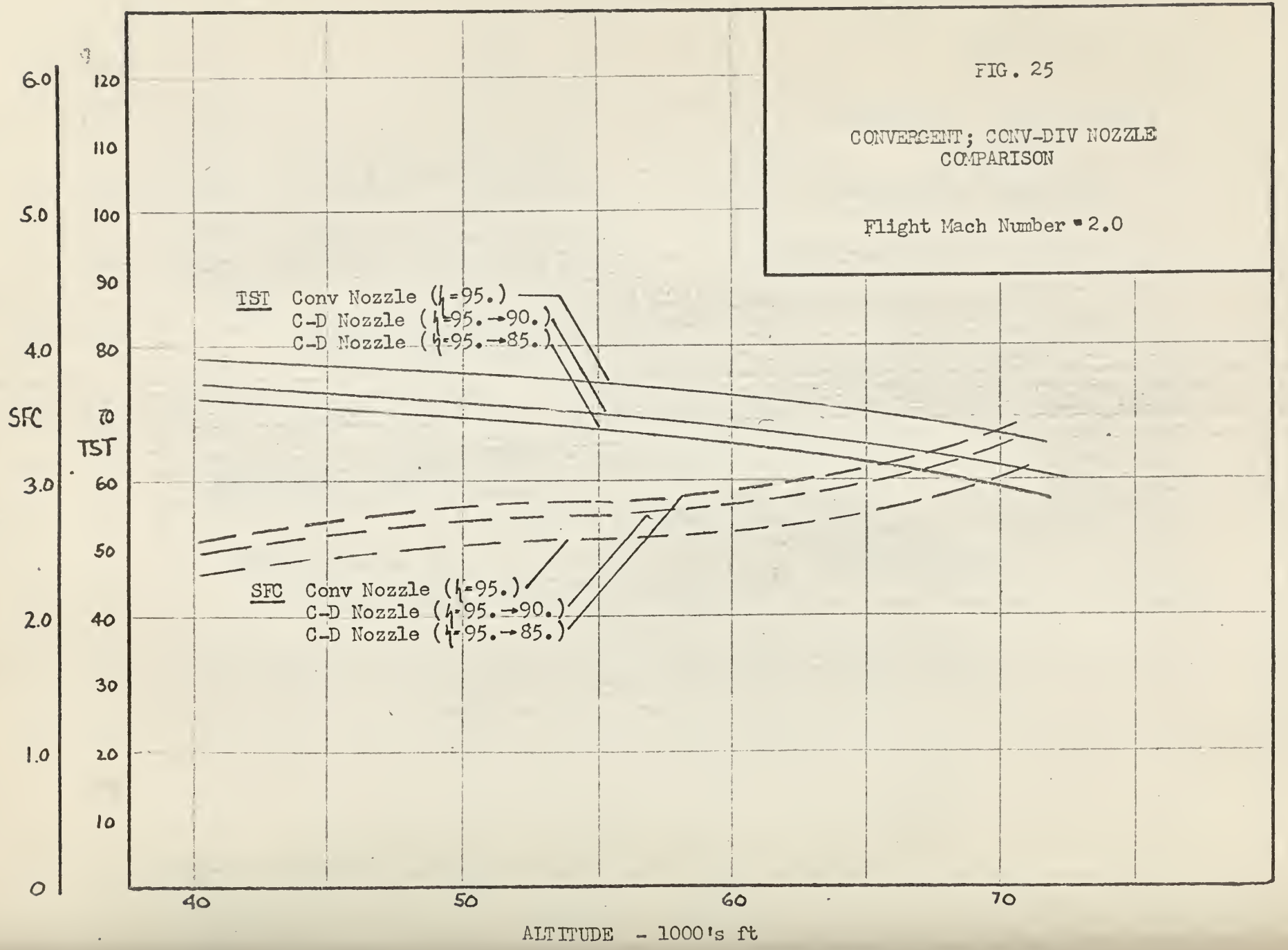
FIG. 25
CONVERGENT; CONV-DIV NOZZLE COMPARISON
Flight Mach Number = 2.0
TST Conv Nozzle (ϕ=95.)
C-D Nozzle (ϕ=95.→90.)
C-D Nozzle (ϕ=95.→85.)
SFC Conv Nozzle (ϕ=95.)
C-D Nozzle (ϕ=95.→90.)
C-D Nozzle (ϕ=95.→85.)
SFC
TST
6.0
5.0
4.0
3.0
2.0
1.0
0
120
110
100
90
80
70
60
50
40
30
20
10
40
50
60
70
ALTITUDE - 1000's ft

FIG. 26

CONVERGENT ; CONV-DIV NOZZLE COMPARISON

Flight Mach Number = 3.0